This manuscript has been accepted for publication in *Annual Review of Microbiology* (2019, vol. 73).

STRUCTURAL BASIS OF RESPONSE REGULATOR FUNCTION

Rong Gao, Sophie Bouillet, Ann M. Stock

Center for Advanced Biotechnology and Medicine, Department of Biochemistry and Molecular Biology, Rutgers – Robert Wood Johnson Medical School, Piscataway, New Jersey 08854, USA; email: rgao@cabm.rutgers.edu, sb1722@cabm.rutgers.edu, stock@cabm.rutgers.edu

Author ORCID Numbers:

Gao: 0000-0002-9245-4952

Bouillet: 0000-0002-0113-3169

Stock: 0000-0002-0446-8079

Corresponding Author: Ann Stock

CABM

679 Hoes Lane West

Piscataway, NJ 08854

+1 848-445-9812

Shortened Title: Response Regulator Structure Function

Keywords

histidine kinase, phosphorylation, response regulator, signal transduction, transcription factor, two-component system

PeerJ Preprints | https://doi.org/10.7287/peerj.preprints.27554v2 | CC BY 4.0 Open Access | rec: 21 Mar 2019, publ: 21 Mar 2019

Abstract

Response regulators function as the output components of two-component systems, which couple the sensing of environmental stimuli to adaptive responses. Response regulators typically contain conserved receiver (REC) domains that function as phosphorylation-regulated switches to control the activities of effector domains that elicit output responses. This modular design is extremely versatile, enabling different regulatory strategies tuned to the needs of individual signaling systems. This review summarizes functional features that underlie response regulator function. An abundance of atomic resolution structures and complementary biochemical data have defined the mechanisms for response regulator enzymatic activities, revealed trends in regulatory strategies utilized by response regulators of different subfamilies and provided insights into interactions of response regulators with their cognate histidine kinases. Among the hundreds of thousands of response regulators identified, variations abound. This article provides a framework for understanding structural features that enable function of canonical response regulators and a basis for distinguishing non-canonical configurations.

PeerJ Preprints | https://doi.org/10.7287/peerj.preprints.27554v2 | CC BY 4.0 Open Access | rec: 21 Mar 2019, publ: 21 Mar 2019

1. INTRODUCTION

Two-component systems (TCSs) are the predominant multi-step signaling pathways in bacteria. Two conserved proteins, a histidine protein kinase (HK) and response regulator (RR), constitute the core system (**Figure 1*a***). Autophosphorylation of the HK at a conserved His provides a high-energy phosphoryl group that is transferred to a conserved Asp in the RR, resulting in RR activation (99). Stimuli, sensed either directly or indirectly by the HK, regulate opposing autophosphorylation/phosphotransfer and RR phosphatase activities of the HK, thus determining the level of phosphorylation of the RR and the output response. A large variety of input domains in HKs and output domains in RRs allows the coupling of an almost limitless array of chemical or physical stimuli to diverse output responses. The conserved proteins and the systems themselves are extremely versatile. An enormous range of variations in protein activities, domain architectures and system configurations allows adaptation of TCSs to the needs of specific signaling systems.

TCSs are found in bacteria, archaea (41) and eukaryotes such as slime molds, yeast, and plants (2). While great diversity exists among all TCSs it should be noted that some specific trends in system configurations are found in different organisms. The Pfam database (35) lists >342,000 entries of proteins containing the conserved receiver (REC, named Response_reg in Pfam) domain that characterizes RRs and >650 structures of such proteins in the Protein Data Bank (PDB) (18). In addition to their presence in RRs, REC domains are also found in hybrid HKs that function within phospho-relay systems involving multiple phosphotransfer steps, accounting for ~10% of REC domain-containing proteins. The scope of this review will focus on bacterial RRs that mediate output of TCSs. Among these RRs, variations abound. The plasticity of the REC domain and the versatility of TCS architecture has driven the evolution of RRs that are uniquely adapted and fine-tuned for function in specific pathways. Out of necessity, this review will focus on canonical RRs with full

PeerJ Preprints | https://doi.org/10.7287/peerj.preprints.27554v2 | CC BY 4.0 Open Access | rec: 21 Mar 2019, publ: 21 Mar 2019

understanding, but lack of specific acknowledgement of individual cases, that for every feature noted, exceptions exist.

This review provides an overview of the structure of RRs and features that provide conserved enzymatic activities in REC domains. Beyond the core domain structures and common enzymatic mechanisms, RRs display great variation in domain arrangements that provide a variety of mechanistically distinct regulatory mechanisms. However, as structures have accumulated, trends in regulatory strategies used by different subfamilies of RRs have begun to emerge and these will be explored in this review.

2. RESPONSE REGULATOR ARCHITECTURE

REC Domains

RRs are defined by the presence of a conserved REC domain. The REC domain fold is composed of five α helices surrounding a central five-stranded parallel β-sheet with a 21345 topology (**Figure 1*b***). Sequence identity between REC domains is usually 20-30%, showing great variations (**Figure 1*c***). The central hydrophobic β-strands, β1, β3, β4 and β5, are more conserved than the peripheral helices and loops. The most conserved residues include the site of phosphorylation, an Asp at the *C*-terminus of β3, and several other residues in the β-α loops, which constitute the active site. The highly conserved phosphorylation site and the variable peripheral sequences allow RRs to couple phosphorylation to diverse effector functions.

Effector Domains

RRs typically function as the output components of signaling pathways. Regulatory REC domains can be linked either covalently or non-covalently to a great diversity of effectors and thus control numerous diverse responses. **Figure 2** summarizes the distribution of the major RR effector domains

PeerJ Preprints | https://doi.org/10.7287/peerj.preprints.27554v2 | CC BY 4.0 Open Access | rec: 21 Mar 2019, publ: 21 Mar 2019

identified in the Pfam database. Approximately one fourth of RRs (23%) consist solely of a REC domain. These single-domain RRs (SDRRs) regulate intermolecular effectors such as the chemotaxis system regulator CheY, which binds to the flagellar motor component FliM controlling flagellar rotation. CheY-like proteins found in chemotaxis-like or chemosensory systems mediate responses other than chemotaxis, for example biofilm formation regulated by Cle proteins (77). Other functions for SDRRs include acting as intermediates in phosphorelays (e.g. the general stress response proteins SdrG and MrrA, and the sporulation protein Spo0F) (45, 63), as phosphate sinks to control phosphate flux within phosphorelays (e.g. *Rhizobium meliloti* CheY1) (97), as allosteric regulators of HKs (e.g. *Caulobacter crescentus* DivK) (24, 117) or as protease adapters (e.g. *C. crescentus* CpdR) (56).

The largest class of RRs (64.5%) is composed of RRs containing a DNA-binding domain (DBD) with subfamilies defined by different DBD folds. The OmpR subfamily (29% of RRs) contains a winged-helix effector domain (68), the NarL subfamily (19%) a four-helix DNA-binding HTH domain (73), the NtrC subfamily (7%) a Fis-type HTH domain fused to an AAA+ ATPase domain and the LytTR (5.5%) a predominantly β fold (94). The abundance of RRs in this class likely reflects the importance of transcriptional regulation as a response to environmental change. A small class of RRs (1%) harbors an RNA-binding domain belonging to the ANTAR subfamily of anti-termination factors such as AmiR (79).

RRs with enzymatic domains account for ~8% of RRs. A major group within this class (3% of RRs) is the regulators of cyclic di-GMP including cyclases (GGDEF) and phosphodiesterases (EAL, HD-GYP) (92). A second major group (2%) is the chemotaxis methylesterase CheB proteins (31). A variety of different enzymatic domains have been identified in other RRs (3%) such as the PP2C phosphatase domain of RsbY and the hybrid kinase domain of FrzE (30, 54). RRs with protein

PeerJ Preprints | https://doi.org/10.7287/peerj.preprints.27554v2 | CC BY 4.0 Open Access | rec: 21 Mar 2019, publ: 21 Mar 2019

binding domains account for ~1% of RRs. Examples in this class include CheV, with a CheW-like domain that connects chemoreceptors to the chemotaxis histidine kinase CheA; RssB, which regulates turnover of the stress response sigma factor RpoS; and PhyR, a regulator of the general stress response that contains an extracytoplasmic function (ECF) sigma factor-like domain (1, 11, 66). While RRs often contain a simple REC-effector domain architecture they can have complex domain organizations with additional signaling domains including PAS, GAF, HisKa, HATPase, etc. The large variety of RRs identified to date emphasizes the versatility of the REC domain with no apparent limits on the types of effector domains that can be controlled by this phosphorylation-activated switch.

3. ENZYMATIC ACTIVITIES OF RRs

Conserved Phosphorylation Site

One of the defining characteristics of the REC domain is its highly conserved phosphorylation site. Due to the lability of the high-energy acyl phosphate, structural characterization of the active site often relies on beryllofluoride (BeF_3^-) that noncovalently binds to the phosphorylation site Asp and serves as a mimic of the phosphoryl group (119). Different BeF_3^--bound RR structures reveal a conserved active site with a network of hydrogen bonds (**Figure 3*a***). The carboxylate side chains of the acidic residue duo (DD) at the β1-α1 loop participate in coordinating a Mg^{2+} required for catalysis. Sidechains of two additional residues, a Thr/Ser (T) at the β4-α4 loop and a Lys (K) at the β5-α5 loop, together with backbone atoms of non-conserved active site residues, coordinate phosphate oxygens in the phosphorylated REC domain.

RR phosphorylation level, the ultimate determining factor of TCS output for canonical RRs, is regulated by multiple enzyme activities, including phosphotransfer from HKs, dephosphorylation

PeerJ Preprints | https://doi.org/10.7287/peerj.preprints.27554v2 | CC BY 4.0 Open Access | rec: 21 Mar 2019, publ: 21 Mar 2019

by auxiliary phosphatases or bifunctional HKs that also possess RR phosphatase activity, autophosphorylation by small-molecule phosphodonors such as phosphoramidate and acetyl phosphate (AcP) (67, 115), and autodephosphorylation activities. Similar phosphorylation sites with almost identical positioning of active site residues have been observed in numerous RR or RR complex structures (21, 81, 86, 107). A pentavalent phosphorus intermediate is believed to be a common transition state for different activities of the REC domain (**Figure 3*b***). Both phosphorylation and dephosphorylation reactions can proceed through either an associative or a dissociative mechanism depending on how tight or extended the transition state is. A phosphodonor or water molecule needs to be in line with the acyl phosphate bond that is to be formed or broken. The phosphotransferase or phosphatase helps position these molecules to further enhance the reaction rates. In all cases, the majority of residues involved in coordinating the phosphorus intermediate are from the REC domain. Thus, most RRs are catalytically competent of autophosphorylation and autodephosphorylation in the absence of any enzymatic protein partner and in vitro analyses of these reactions often provide insights into RR regulatory mechanisms.

Autodephosphorylation and Autophosphorylation

Despite the highly conserved active site geometry, RRs show large variations in rates of autophosphorylation and autodephosphorylation (87, 101, 102). For example, autodephosphorylation rate constants of the REC domain range over six orders of magnitude, giving phosphorylation half-lives of seconds to hours and even days (101). Such great diversity is partly attributed to several variable residues surrounding the active site, such as positions D+2 (two residues *C*-terminal to the conserved D), T+1 and T+2 (one and two residues *C*-terminal to T) (**Figure 3*b* and 3*c***). Backbone atoms of D+2 and T+1 directly form hydrogen bonds with the phosphoryl group while the charge, size and hydrophobicity of sidechains at these three positions may affect the energy barrier of the

PeerJ Preprints | https://doi.org/10.7287/peerj.preprints.27554v2 | CC BY 4.0 Open Access | rec: 21 Mar 2019, publ: 21 Mar 2019

transition state, facilitate the positioning or block the in-line path of the phosphodonor or attacking water (53, 80, 102, 121). In more than half of RR sequences, a limited number of amino acid combinations are preferred at these positions and the distribution of preferred amino acids correlates with RR effector subfamilies (53, 80). REC enzyme activities are therefore suggested to co-evolve with effector domain regulation and these residues represent functional sites for modulating the stability of RR phosphorylation to match the timescale of individual TCS output responses.

Phosphorylation by small molecules, particularly AcP, has long been suggested to be physiologically relevant in some RRs to couple TCS output to global conditions (115). RR phosphorylation, often in the absence of the cognate HK, can be influenced by cellular AcP levels that are sensitive to the metabolic state of cell. Because the phosphorylation rate by AcP is usually much slower than the rate of phosphotransfer by the cognate HK and often offset by the phosphatase activity of bifunctional HKs or other auxiliary phosphatases (43, 57), the contribution of phosphorylation by AcP to TCS output is typically minimal in wild-type cells. However, given the great diversity of TCSs, AcP can play a significant role in some systems, specifically those with a fast RR autophosphorylation rate and/or a slow phosphatase rate (59, 85).

HK-mediated Activities

RR phosphatase activities mediated by HKs or auxiliary phosphatases are believed to function through positioning a water molecule and stimulating the intrinsic RR autophosphatase activity (17). Structure of CheY3 complexed with the phosphatase CheX (86) reveals an amide side chain inserting into the RR active site and forming a hydrogen bond with the attacking water molecule (**Figure 3*c***). Similar positioning of the amide from a Gln or Asn residue has been observed in different phosphatases with distinct structures, such as CheX (86), CheZ (123) and RapH (81), as well as the phosphatase state of DesK, a bifunctional HK from the second largest HK subfamily,

PeerJ Preprints | https://doi.org/10.7287/peerj.preprints.27554v2 | CC BY 4.0 Open Access | rec: 21 Mar 2019, publ: 21 Mar 2019

HisKA_3 (107). The Gln-containing sequence motif, DXXXQ, is located immediately after the phospho-accepting His residue in HKs from the HisKA_3 subfamily. The His residue does not appear to be required for RR dephosphorylation despite its close proximity to the phosphatase-essential Gln (52) . For the largest HK subfamily, HisKA, the His residue may play a role in RR dephosphorylation (62, 125) but the exact phosphatase mechanism is less clear. An EXXN/T motif similar to CheX-like phosphatases has been identified and the conserved Asn/Thr residue is suggested to be the catalytic residue (52). However, among the available structures of RR complexes with HKs of the HisKA subfamily, the side chain of the Asn/Thr residue is not at a similar position as the Asn/Gln in other phosphatases and is distant from the active site Asp. A dual engagement model has been suggested involving both His and Asn/Thr residues positioning the catalytic water molecule (62). Roles of the two residues may differ for individual HisKA proteins depending on structural details and structures unequivocally capturing the phosphatase state are needed to elucidate the mechanism.

Loss of RR phosphorylation can result from autodephosphorylation, dephosphorylation by the HK and back-transfer to the cognate HK (34, 98), i.e. the reverse reaction of phosphotransfer. The back-transferred histidyl phosphoryl group can be further transferred to ADP (46, 100) or to other RRs that function as phosphate sinks to modulate phosphorylation levels (3, 98, 103). Back-transfer is suggested to accompany an associative transfer mechanism that has a tight RR phosphorylation transition state and appears to be evolved for bi-directional transfer common in CheA or other HPt-containing phosphorelay proteins (107, 122). Unidirectional phosphotransfer with little back-transfer, observed in several canonical HKs, is linked to a dissociative mechanism and the asymmetry of the Mg^{2+} position in an extended transition state (107). The dissociative mechanism can be distinguished by a long distance between the conserved Asp and His residues in

PeerJ Preprints | https://doi.org/10.7287/peerj.preprints.27554v2 | CC BY 4.0 Open Access | rec: 21 Mar 2019, publ: 21 Mar 2019

an HK-RR complex structure. It remains to be investigated whether there is any domain preference or sequence signature that distinguishes the two mechanisms and determines the relative rates of forward- and back-transfer. Residues affecting the transition state stability, such as non-conserved residues at D+2, T+1 and T+2 positions, also modulate the HK-catalyzed phosphotransfer rate (53, 107). Due to multiple phosphorylation and dephosphorylation reactions present simultaneously, quantitation of individual activities is often complicated by interference from other activities. Furthermore, RR activities measured *in vitro* with truncated cytoplasmic fragments of transmembrane HKs require careful examination and may differ greatly from their full-length counterparts in the cellular environment (43).

4. REGULATORY MECHANISMS IN RR SUBFAMILIES

As a phosphorylation-activated switch between inactive and active conformations, the REC domain mediates effector functions through intramolecular and/or intermolecular interactions. Structures of individual REC and effector domains usually undergo subtle changes upon phosphorylation, but the overall structures may vary greatly because of different domain arrangements. A typical RR regulatory mechanism is exemplified by *Staphylococcus aureus* VraR (**Figure 4*a*)**, one of a few RRs with full-length protein structures available in both phosphorylated (or BeF_3^--bound) and unphosphorylated states (60). The monomeric unphosphorylated VraR adopts a closed conformation with extensive contacts between the REC and DBD effector domains, holding the DNA-recognition helix at a position unfavorable for dimerization on DNA. Phosphorylation results in an extended conformation with a flexible linker between the two domains and an altered REC surface that promotes RR dimerization for DNA binding.

PeerJ Preprints | https://doi.org/10.7287/peerj.preprints.27554v2 | CC BY 4.0 Open Access | rec: 21 Mar 2019, publ: 21 Mar 2019

Negative regulation in the inactive state and positive regulation in the active state, as shown for VraR, are two common mechanisms mediated by the REC domain (**Figure 4*b***). For positive regulation, the REC domain facilitates the effector domain function, as shown for many DBD-containing RRs in which dimerization of the phosphorylated REC domains is thought to promote DNA binding and transcription regulation. Effector domains of some RRs, such as NtrC1 (58) and CheB (31), are catalytically competent when alone, but are inhibited by the REC domain in the inactive state. The two mechanisms are not exclusive and many RRs use both. Regulatory details for individual RRs show great variations that may have been evolved to adapt each protein to its unique structure and function. For example, in inactive states, interactions between REC and effector domains can differ dramatically (**Figure 4*b***), even within the same subfamily of RRs (42). Functional sites, such as the DNA-recognition helix for DBDs and the active site for enzymatic effector domains, can be buried within the REC-effector interface or exposed but held at unfavorable positions by tight interactions. Extended conformations with few interdomain contacts have also been observed for a few RRs that are believed to employ a positive regulatory mechanism.

Inactive and Active Conformational States

The REC interaction surface that mediates effector domain function is usually distant from the phosphorylation site. A dynamic allosteric mechanism allows conformational changes at the phosphorylation site to propagate to the distal interaction surface. The REC domain samples different allosteric conformations and exists in equilibrium between inactive and active conformations, with phosphorylation shifting the equilibrium. A “Y-T coupling” allosteric mechanism was initially described for CheY (25, 124) and several other RRs (14, 47). Rearrangement of the conserved T at the phosphorylation site (**Figure 3*a***) is believed to correlate with the rotameric conformation of a conserved Tyr/Phe (Y) residue in the β5 strand. In the active

PeerJ Preprints | https://doi.org/10.7287/peerj.preprints.27554v2 | CC BY 4.0 Open Access | rec: 21 Mar 2019, publ: 21 Mar 2019

248 state, the aromatic side chain is oriented toward the interior of the REC domain, distinct from the
249 outward position in the inactive state (**Figure 5*a***), resulting in alteration of the α4-β5-α5 face, a
250 surface widely used by many RRs for interdomain interactions. Because of the readily recognizable
251 position of the two residues, they are often used to classify structures as inactive or active, with the
252 caveat that the conformational change involves a broad surface of the REC domain and Y-T
253 coupling is not the only allosteric mechanism (20, 109).

254 X-ray crystallography has been central to understanding RR regulatory mechanisms although
255 conformations trapped in crystals represent only static snapshots of RR conformational dynamics
256 and can be influenced by experimental conditions, crystal lattice contacts and high protein
257 concentrations used in crystallization. A particular interaction interface or
258 dimerization/oligomerization mode observed in crystal structures, such as domain-swapped dimers
259 observed in several RRs (17, 26, 55), may not be physiologically relevant and requires
260 complementary experiments for validation. Nevertheless, an increasing number of RR structure
261 snapshots start to reveal different states of conformational trajectories and trends of prevalent
262 regulatory strategies in RR subfamilies.

263 DBD-containing RRs, the largest class of RRs, have the greatest number of X-ray structures
264 available, making it possible to analyze the allosteric conformational features within individual RR
265 subfamilies (**Table 1**). All structures crystalized with phosphorylated or BeF_3^--bound RRs display
266 inward orientations of the side chain at the conserved Y position while conformations of
267 unphosphorylated RRs are diverse. For unphosphorylated RRs in the OmpR and NtrC subfamilies,
268 both outward and inward orientations of Y residues have been observed, with the inward orientation
269 more readily observed for the REC domain alone than for multi-domain proteins (**Table 1**). This is
270 consistent with NMR studies suggesting that unphosphorylated RRs exist in equilibrium between

PeerJ Preprints | https://doi.org/10.7287/peerj.preprints.27554v2 | CC BY 4.0 Open Access | rec: 21 Mar 2019, publ: 21 Mar 2019

inactive and active conformations (110) while interactions with the effector domain shift the equilibrium to the inactive state (27). The inward orientation of Y is predominant for most NarL subfamily members irrespective of phosphorylation status, thus is unlikely indicative of the active state, but rather a result of packing the α4-β5-α5 face with an accessory β6 strand, a structural feature found in many RRs of the NarL subfamily (20, 60, 83, 106). Therefore, the Y-T coupling mechanism is not universal in all RRs. Even for NtrC in which orientation switching has been observed, interconversion of the aromatic side chain has been suggested not to be involved in allosteric regulation because its rate of conversion is faster than the rate of active/inactive state conversion (109). RRs appear to be highly plastic for allosteric regulation with diverse mechanisms matching their sequence and structural features.

The Y and T residues are two of many residues that may participate in allosteric regulation. As discussed earlier, the phosphorylation site involves an intricate hydrogen-bond network with several residues from the β1-α1, β3-α3, β4-α4 and β5-α5 loops. It has been recognized that interactions, such as salt bridges and van der Waals contacts, of residues at D+1, T+1, T+2, K and other positions can impact loop conformations and propagate the conformational changes to different areas of the REC domain (5, 14, 20, 44, 70, 106). Conformations with only subsets of active site residues at proper hydrogen-bonding positions have been discovered for many RRs (37, 95, 106) and are often referred to as meta-active states. A single RR can have multiple meta-active states with different combinations of loop conformations, as shown for NtrX (37). Unphosphorylated RRs can exist in equilibrium between the active state and multiple inactive or meta-active conformations and there are multiple pathways for transition to the active state (37, 44, 89). NMR relaxation data also support a model of segmental motions of multiple allosteric residues for activation of CheY, instead of a strict two-state switching model (70).

PeerJ Preprints | https://doi.org/10.7287/peerj.preprints.27554v2 | CC BY 4.0 Open Access | rec: 21 Mar 2019, publ: 21 Mar 2019

Just as phosphorylation shifts the equilibrium for effector domain regulation, the reverse scenario, with output domains affecting phosphorylation, has also been observed (8, 37). It has been suggested that adoption of an active conformation precedes phosphorylation (44, 53). Phosphorylation can be accelerated by any effect that increases the population of active conformation, such as relieving inhibition from the output domain by truncation, DNA binding in DBD-containing RRs, dimerization at high protein concentrations and HK-RR interaction (8, 9, 27, 28, 37, 66). Surface changes caused by these different interactions can propagate through the connecting βα loops to the phosphorylation site and other regions of the REC domain, increasing the active state population. One extraordinary example is DesR in which the HK-RR interaction can stabilize the active state of DesR and promote dimerization (66). Besides the phosphorylation-activated switch, interaction with the HK also functions as an allosteric switch to increase the population of active conformation for transcription activation. The same principle may be the basis for many phosphorylation-independent regulatory mechanisms.

Dimerization Modes and Corresponding Conformational Changes

Phosphorylation-promoted conformational changes are routinely identified by comparing X-ray or NMR structures obtained for unphosphorylated and BeF_3^--bound RRs. As shown in **Figure 5*a***, for the stand-alone RR CheY, significant differences in positions of backbone atoms occur at the β4-α4, β5-α5 loops and part of the α4-β5-α5 surface where CheY binds the FliM effector protein to regulate flagellar rotation. It is unsurprising that structural elements of the REC domain undergoing the largest rearrangements upon phosphorylation often correlate with protein-protein interaction surfaces, particularly, the dimer interface for DBD-containing RRs. Certain dimerization modes are popular for specific RR subfamilies with corresponding conformational changes.

PeerJ Preprints | https://doi.org/10.7287/peerj.preprints.27554v2 | CC BY 4.0 Open Access | rec: 21 Mar 2019, publ: 21 Mar 2019

A dimerization mode using the complete α4-β5-α5 surface is predominant in the OmpR subfamily (**Figure 5*b***). Dimer interaction involves salt bridges between pairs of highly conserved charged residues within the α4-β5-α5 region (104, 105). For the DrrB protein shown in **Figure 5*b***, conformational changes span the entire dimer surface. A Tyr residue is prevalent at the Y position (111) and switching of Tyr orientations has been observed. In several RRs (40, 78, 91), the hydroxyl group of Tyr is in close proximity to a polar residue from the DBD (**Figure 5*b right***), suggesting a potential role in effector inhibition. This is unlikely to be a common mechanism given the wide diversity of domain arrangements within the subfamily (8). RRs from the OmpR subfamily often recognize tandem DNA sites and two DBDs bind DNA in a head-to-tail manner (15, 48, 64, 76). The translational symmetry of DBDs coupled with the rotational symmetry of the REC domain predicts a flexible linker or different REC-DBD interfaces for individual RR monomers within the RR-DNA complex. Such asymmetry of REC-DBD interfaces has been observed for KdpE and PmrA (65, 76). However, NMR studies suggest that the REC-DBD interaction observed for PmrA in the crystal structure is transient in solution (65). Additionally, alternative dimers involving α1-α5 (6, 71) or other surfaces (13) have also been discovered for unphosphorylated RRs but the physiological relevance of these dimers awaits further studies.

The NtrC subfamily of RRs displays two major modes of dimerization, with each involving different subsets of the α4-β5-α5 face (**Figure 5*c***). The α4-β5 dimer interface is often seen in phosphorylated RRs (**Table 1**) or unphosphorylated RRs with meta-active conformations (32, 37, 84). Another β5-α5 dimer is associated with inactive conformations (36, 84), as indicated by the outward orientation of the Phe residue at the Y position. Dimer interaction centers around the β5-α5 face, sometimes with a slightly tilted α5 helix in contact with both β5 and α4. Formation of the inactive β5-α5 dimer is believed to inhibit the AAA,+ ATPase output domain from oligomerization

PeerJ Preprints | https://doi.org/10.7287/peerj.preprints.27554v2 | CC BY 4.0 Open Access | rec: 21 Mar 2019, publ: 21 Mar 2019

and transcription initiation (10, 84). For the LytTR subfamily, structural information is limited and a dimer also involving the α4-β5 subset of the α4-β5-α5 face has been observed for ComE (16).

Diverse dimerization modes have also been observed in the NarL subfamily. An α4-β5 dimer interface and the phosphorylation-dependent orientation of the Phe residue have been reported for the REC domain of FixJ (14). However, most RRs from the NarL subfamily show an α1-α5 dimer interface (**Table 1**) distinct from the widely used α4-β5-α5 surface (7, 20, 29, 60, 82, 106). The dimer interface mainly involves the α1 helix, the β1-α1 and β5-α5 loops (**Figure 5*d***). Correspondingly, significant structural rearrangements spanning to the α1 helix have been observed when apo- and BeF_3^--bound structures are compared. As discussed earlier, many RRs of the NarL subfamily display a constitutive inward orientation of the residue at the Y position, thus this residue is unlikely to be involved in allosteric regulation. Instead, different switching mechanisms involving the T residue and other residues at α1, the β1-α1, β4-α4 and β5-α5 loops have been proposed for different RRs, such as VraR, DesR and RcsB (20, 60, 106). In addition to the α1-α5 dimer interface, the α4-β5-α5 surface is also remodeled to alter the positioning of the accessory β6 and α6 that are directly linked to the effector domain. Another dimer mode involving β6 and α6 is common (**Figure 5*d, right***) and several RRs, such as VraR (60), DesR (106), Spr1814 (82) and LiaR (29), show both α1-α5 and β6-α6 dimer modes within a single crystal. It has been suggested that the β6-α6 dimer may help RRs to form higher order oligomers on DNA to bind arrays of DNA-binding sites (106). DNA-bound structures of RcsB again indicate an asymmetric dimer with different rotation symmetry axes for the REC and DBDs (38). Different relative positions of the REC and DBDs are frequently observed for different full length RRs. Asymmetry is believed to result from either different REC-DBD interactions (20, 38) or a flexible linker that enables different disposition or even domain-swap of individual domains trapped in crystals (29, 60).

PeerJ Preprints | https://doi.org/10.7287/peerj.preprints.27554v2 | CC BY 4.0 Open Access | rec: 21 Mar 2019, publ: 21 Mar 2019

5. RESPONSE REGULATOR – HISTIDINE KINASE INTERACTIONS

HK Conformational States

HKs have a modular architecture with a large variety of sensory domains (extracellular, transmembrane or cytoplasmic) linked to a conserved catalytic domain by one or more signal transducing domains (12, 69) (**Figure 1*a***). The cytoplasmic enzymatic core of HKs consists of a dimerization histidine phosphotransfer (DHp) domain and a catalytic ATP-binding (CA) domain. The DHp domain contains the conserved phosphorylatable His residue and mediates dimerization of the HK to form a 4-helix bundle that is essential for its activity (**Figure 6**). The DHp dimer is flanked by the two α/β catalytic CA domains containing the kinase active sites that catalyze phosphoryl transfer from ATP to the His residues. Autophosphorylation of the HK provides a high-energy phorphoryl group for subsequent phosphotransfer to the RR. Most HKs also mediate dephosphorylation of their cognate RRs in order to modulate the output response.

Large conformational changes in HKs occur during transitions between kinase, phosphoryltranfer and phosphatase states. In the HisKA_3 subfamily of HKs (e.g. DesK of *Bacillus subtilis*), the switch between states involves a large rotation of the DHp domains, a mechanism that is less pronounced in the HisKA subfamily. Specific regulatory mechanisms have been described for individual HKs, including the stabilization of the phosphatase state by ligand binding (e.g. c-di-GMP binding on CckA) and the inhibition of the phosphatase state by a pH-dependent conformational switch (33, 62). In contrast to the different conformations of HKs, structures of HK-REC domain complexes determined to date indicate that REC domains bound to either phosphotransfer or phosphatase states of HKs have similar conformations, with the REC domain displaying a meta-active conformation, as defined in the previous section.

PeerJ Preprints | https://doi.org/10.7287/peerj.preprints.27554v2 | CC BY 4.0 Open Access | rec: 21 Mar 2019, publ: 21 Mar 2019

Partner Recognition and Specificity

Specificity of HK-RR pairs is crucial for the integrity of signaling pathways, given the large number of different TCSs that typically exist in a single cell. Specificity within a pair is mediated by recognition residues that participate in HK-RR binding. These residues are located in helix α1 of the REC domain and in the two α helices of the HK DHp domain that contribute to the binding interface. Signaling pathways have been successfully rewired by substituting as few as three co-evolved specificity residues (88, 96). Additional strategies are employed to further ensure specificity of the pairs. For example, the phosphatase activity of HKs eliminates non-specific phosphorylation by non-cognate kinases or small molecule phosphodonors such as AcP. The low-abundance of HKs relative to RRs also minimizes cross-phosphorylation between non-cognate pairs (57).

In an HK-RR complex, the REC domain inserts its α1 helix and β5-α5 loop between the two helices of the DHp domain, primarily contacting the DHp α1 helix that contains the phosphorylatable His residue. This conserved mode of binding buries the active site of the REC domain at the HK-RR interface (**Figure 6**). Thus, conserved residues of both the HK and RR form a substantial subset of the interface residues, with specificity being determined by a relatively small set of variable residues. In addition to these specificity residues in α1 of the REC domain and the two helices of the DHp domain, additional variable contacts can involve the β2-α2, β3-α3 and β4-α4 loops of the REC domain interacting with the CA domain, the *C*-terminal region of the DHp and the DHp-CA linker of the other protomer of the dimer (**Figure 6**) (21, 72, 74, 88, 107, 108, 114, 118, 122). Other contacts can occur between the REC domain and additional domains within the HK, increasing the specificity and/or stability of the pair (e.g. contacts between the PAS domain of ThkA and the RR TrrA) (118). These elements suggest that beyond the conserved REC-DHp interface that buries the active site, the binding interface can vary greatly in different HK-RR pairs.

PeerJ Preprints | https://doi.org/10.7287/peerj.preprints.27554v2 | CC BY 4.0 Open Access | rec: 21 Mar 2019, publ: 21 Mar 2019

A model based on structures of HK FixL and full-length RR FixJ suggests that the RR effector domain is free to move and does not participate in binding to the HK (116). However, a lack of structures of full-length RRs bound to HKs leaves open the question as to how effector domains might be positioned relative to REC domains and domains of the HK. Given the great diversity in REC-effector domain arrangements in different inactive RRs, it is possible that diversity exists in the ways effector domains interact in different HK-RR complexes. It is easy to envision how an effector domain could participate in the stability of the complex and/or the efficiency of catalysis. Indeed, the meta-active conformation of the REC domain observed in HK-REC domain complexes might be a consequence of isolated REC domains being unhindered by REC-effector interactions that could bias conformational states.

Phosphotransfer State

Structural and biochemical studies of DesK-DesR complexes suggest that one HK dimer binds to one RR molecule in an asymmetric conformation. The DesK-DesR structure and a docking model of CpxA-CpxR in a putative phosphotransfer state show asymmetry within the HK dimer, with the CA domain of one monomer bound to the DHp domain of the other monomer, leaving the second CA domain untethered with enough space for RR binding to the DHp. Structural data from the DesK-DesR complex and from CpxA-CpxR model suggest that this highly dynamic state is coupled with autokinase activity, involves back-and-forth movements of the DHp and CA domains, and is modulated by REC domain binding (72, 107).

Phosphatase State

In contrast to the asymmetrical domain arrangements associated with phosphotransfer, HK-RR complexes in putative dephosphorylation states have symmetrical arrangements of the HK DHp and CA domains. The REC domains are also arranged symmetrically, each interacting with a DHp

PeerJ Preprints | https://doi.org/10.7287/peerj.preprints.27554v2 | CC BY 4.0 Open Access | rec: 21 Mar 2019, publ: 21 Mar 2019

domain with a 2:2 HK:RR stoichiometry (62, 107). The HK in its phosphatase state is more rigid than in the phosphotransfer state, with the *N*-terminal coiled-coil of the DHp domains being highly stable.

Despite the large number of structures recently determined, the mechanistic details of the enzymatic reactions involving HKs and RRs are not fully understood. Discrimination between the phosphotransfer and phosphatase states that have been trapped in crystal structures still remains challenging. The situation is further complicated by distinct phosphatase mechanisms used by HKs of different subtypes. A major limitation of current studies is the use of truncated proteins, most notably the cytoplasmic domains of transmembrane HKs lacking sensor and transmembrane regions that in intact proteins control the signaling states of HKs, and REC domains of RRs in the absence of effector domains that are known to influence their conformational equilibria. While conserved features of HK-RR interactions are beginning to be elucidated, variations on the theme are anticipated. Similar to many other aspects of TCS structure and function, it is likely that the great variety of domain architectures in TCS proteins enable different modes of HK-RR interactions and regulatory mechanisms that are adapted to individual HK-RR pairs.

6. NON-CANONICAL MODES OF RR REGULATION

The canonical mechanism for regulation of RR activity involves phosphorylation at a conserved Asp in the REC domain, stabilizing an active conformation that enables effector domain function. Regulation of RR activity, in addition to or in place of Asp phosphorylation, potentially can be achieved in many different ways including post-translational modifications at other sites that bias the conformational equilibrium of the REC domain or directly alter effector domain function, interactions that lower the energetic barrier for transition to an active conformation, ligand binding

PeerJ Preprints | https://doi.org/10.7287/peerj.preprints.27554v2 | CC BY 4.0 Open Access | rec: 21 Mar 2019, publ: 21 Mar 2019

454 to the RR, and regulation of expression to control RR levels and thus dimerization or
455 oligomerization. Indeed, each of these strategies has been observed and a few examples are
456 described below.

457 Reversible protein acetylation is known to regulate metabolic enzymes and transcription in
458 bacteria (49) and was documented in CheY more than 20 years ago (90). Enzyme catalyzed
459 acetylation of CheY at K91 and K106 increases in response to acetate and promotes clockwise
460 flagellar rotation, with acetylation at K91 proposed to alter conformational dynamics of the β4α4
461 loop (39). Autoacetylation with AcCoA as acetyl donor at other sites in CheY is thought to link
462 chemotaxis to the metabolic state of the cell (120). Another well-characterized example of
463 acetylation occurs in *E. coli* transcription factor RcsB. Acetylation of K154, a residue in the helix-
464 turn-helix motif that interacts with a phosphate in the DNA backbone, disrupts DNA binding, down-
465 regulates expression of the acid stress response genes, and compromises survival in acidic conditions
466 (22, 51). It should be noted that the stoichiometry of acetylation has not been determined, thus
467 physiological effects observed with mutations that mimic fully unmodified or acetylated states might
468 overestimate regulation that occurs in wild-type cells. A proteomics study in *E. coli* documented
469 acetylation of seven RRs: ArcA, CheY, CpxR, EvgA, NarL, OmpR and RcsB (22). The *E. coli*
470 genome encodes 26 putative Gcn5 *N*-acetyltransferases (GNATs) and a single known deacetylase
471 (CobB) (49). While the best-characterized acetyltransferase, PatZ, is proposed to mediate a global
472 strategy linking regulation to metabolic state, the large number of acetyltransferases raises the
473 possibility of substrate specificity that might enable system-specific signaling mechanisms.

474 Signal-induced, HK-dependent, phosphorylation-independent monomer to dimer activation
475 has been observed for several RR transcription factors. In the extensively studied *B. subtilis* system,
476 binding of DesR to DesK promotes an active conformation of DesR. At sufficiently high RR

PeerJ Preprints | https://doi.org/10.7287/peerj.preprints.27554v2 | CC BY 4.0 Open Access | rec: 21 Mar 2019, publ: 21 Mar 2019

concentrations and with a slow active to inactive state transition, dimerization can occur upon release of the RR from the HK with subsequent stabilization of the dimer upon DNA binding (106). Similar phosphorylation-independent activation of OmpR by HK EnvZ has been observed in acidic conditions (23). Cyanobacterial transcription factor NblR contains a conserved Asp, but lacks other residues necessary for phosphorylation. HK NblS is required for phosphorylation-independent activation of NblR. However, no NblS-NblR interactions have been detected and the activating monomer to dimer transition is postulated to be promoted by another protein partner (93).

Multiple strategies have been identified for regulation of orphan RRs that lack a conserved Asp and/or other conserved residues necessary for phosphorylation. In streptomycetes, two atypical RR transcription factors that lack residues necessary for phosphorylation, JadR1 and RedZ, are regulated by the end products of the antibiotic biosynthetic pathways they control. The antibiotic JdB binds directly to the JadR1 REC domain, disrupting DNA binding (112). A different strategy is used by *Helicobacter pylori* HP1043, which exists as a constitutively active dimer *in vitro* with a crystal structure similar to that of other activated OmpR subfamily members (50). Levels of HP1043 are regulated both transcriptionally and post-transcriptionally leading to speculation that control of expression of this constitutively active RR may be the sole mechanism for regulating HP1403 activity (75).

Combinations of these mechanisms create even more strategies. *Streptomyces coelicolor* GlnR, which regulates genes for nitrogen assimilation, is an orphan OmpR subfamily RR that lacks residues for Asp phosphorylation and forms a constitutive α4-β5-α5 dimer (61). GlnR is phosphorylated at 6 Ser/Thr sites in the DNA-binding domain under N-rich conditions, disrupting DNA binding. GlnR is also acetylated at multiple Lys residues in the DNA-binding domain, with acetylation enhancing DNA binding (4).

PeerJ Preprints | https://doi.org/10.7287/peerj.preprints.27554v2 | CC BY 4.0 Open Access | rec: 21 Mar 2019, publ: 21 Mar 2019

7. CONCLUDING REMARKS

When the structure of an RR REC domain was first reported thirty years ago, a central question was how this single conserved domain could regulate responses as diverse as flagellar rotation, transcription, and enzyme activity. The answer that emerged defined a mechanism that was both simple and versatile. The small α/β REC domain exists in equilibrium between two primary conformations with phosphorylation stabilizing an active conformation. This phosphorylation-regulated switch enables regulatory strategies via any type of activating or inhibitory macromolecular interactions that discriminate between the two states. Hundreds of structures of RRs have provided descriptions of the conformations of REC domains in inactive and active states, interactions with effector domains, DNA, HKs and auxiliary proteins. These structures provide a foundation for identifying conserved features as well as specific variations in individual RRs. Beyond the universally conserved enzymatic mechanisms facilitated by configurations at the active site, other features such as Y-T coupling, regions of conformational perturbations, domain arrangements and modes of DNA binding show distinct trends among RRs within specific subfamilies.

Numerous variations on most every feature of RRs have been observed and undoubtedly, many more remain to be discovered. The plasticity of the REC domain and versatility of RR design allow an almost unlimited array of adaptations to fit the needs of individual signaling systems. Defining details of how specific structural features impact function is important for interpreting the nuances of RR behavior within specific TCSs as well as for pursuit of applied projects such as development of antimicrobial therapeutics or the engineering of synthetic biosensing pathways.

PeerJ Preprints | https://doi.org/10.7287/peerj.preprints.27554v2 | CC BY 4.0 Open Access | rec: 21 Mar 2019, publ: 21 Mar 2019

Our current understanding of RR structure is largely informed by compiling information derived from many partial structural descriptions of different RRs. Very few structures are available for full-length multi-domain RRs in both inactive and active states. The crystal structures that do exist are constrained by the limitations of the methodology, specifically the capture of single discrete states that do not reflect conformational distributions and the potential promotion of inter- and/or intra-molecular interactions that are influenced by the high concentrations of proteins used in crystallization and/or stabilization of conformations necessary for crystallization and lattice interactions. While NMR studies have provided information about dynamics and conformational distributions in solution, size limitations have mostly precluded studies of full-length RRs, dimers, oligomers and complexes of RRs with HKs or other macromolecular partners. Thus, while structures unambiguously define allowable states, it is important to keep in mind the conformationally dynamic nature of RRs and the potential influence of associated domains and macromolecular partners when interpreting structures determined by methodologies with technical limitations. The emergence of new structural methods such as high-resolution cryo-electron microscopy promise to provide solutions to some of these challenges.

DISCLOSURE STATEMENT

The authors are not aware of any affiliations, memberships, funding, or financial holdings that might be perceived as affecting the objectivity of this review.

ACKNOWLEDGMENTS

PeerJ Preprints | https://doi.org/10.7287/peerj.preprints.27554v2 | CC BY 4.0 Open Access | rec: 21 Mar 2019, publ: 21 Mar 2019

543 Research in the Stock laboratory is supported by grant R01 GM47958 from the National Institutes of
544 Health. S.B. was supported in part by the Foundation pour la Recherche Médicale (FRM) Grant
545 SPE201803005070.

546

547

548 **LITERATURE CITED**

549 1. Alexander RP, Lowenthal AC, Harshey RM, Ottemann KM. 2010. CheV: CheW-like coupling
550 proteins at the core of the chemotaxis signaling network. *Trends Microbiol.* 18:494-503
551 2. Alvarez AF, Barba-Ostria C, Silva-Jimenez H, Georgellis D. 2016. Organization and mode of
552 action of two component system signaling circuits from the various kingdoms of life. *Environ.*
553 *Microbiol.* 18:3210-26
554 3. Amin M, Kothamachu VB, Feliu E, Scharf BE, Porter SL, Soyer OS. 2014. Phosphate sink
555 containing two-component signaling systems as tunable threshold devices. *PLoS Comput. Biol.*
556 10:e1003890
557 4. Amin R, Franz-Wachtel M, Tiffert Y, Heberer M, Meky M, et al. 2016. Post-translational
558 serine/threonine phosphorylation and lysine acetylation: a novel regulatory aspect of the global
559 nitrogen response regulator GlnR in *S. coelicolor* M145. *Front. Mol. Biosci.* 3:38
560 5. Amor BR, Schaub MT, Yaliraki SN, Barahona M. 2016. Prediction of allosteric sites and
561 mediating interactions through bond-to-bond propensities. *Nat. Commun.* 7:12477
562 6. Bachhawat P, Swapna GV, Montelione GT, Stock AM. 2005. Mechanism of activation for
563 transcription factor PhoB suggested by different modes of dimerization in the inactive and
564 active states. *Structure* 13:1353-63
565 7. Baikalov I, Schröder I, Kaczor-Grzeskowiak M, Grzeskowiak K, Gunsalus RP, Dickerson RE.
566 1996. Structure of the *Escherichia coli* response regulator NarL. *Biochemistry* 35:11053-61
567 8. Barbieri CM, Mack TR, Robinson VL, Miller MT, Stock AM. 2010. Regulation of response
568 regulator autophosphorylation through interdomain contacts. *J. Biol. Chem.* 285:32325-35

PeerJ Preprints | https://doi.org/10.7287/peerj.preprints.27554v2 | CC BY 4.0 Open Access | rec: 21 Mar 2019, publ: 21 Mar 2019

9. Barbieri CM, Wu T, Stock AM. 2013. Comprehensive analysis of OmpR phosphorylation, dimerization, and DNA binding supports a canonical model for activation. *J. Mol. Biol.* 425:1612-26

10. Batchelor JD, Doucleff M, Lee CJ, Matsubara K, De Carlo S, et al. 2008. Structure and regulatory mechanism of *Aquifex aeolicus* NtrC4: variability and evolution in bacterial transcriptional regulation. *J. Mol. Biol.* 384:1058-75

11. Battesti A, Majdalani N, Gottesman S. 2011. The RpoS-mediated general stress response in *Escherichia coli*. *Annu. Rev. Microbiol.* 65:189-213

12. Bhate MP, Molnar KS, Goulian M, DeGrado WF. 2015. Signal transduction in histidine kinases: insights from new structures. *Structure* 23:981-94

13. Birck C, Chen Y, Hulett FM, Samama JP. 2003. The crystal structure of the phosphorylation domain in PhoP reveals a functional tandem association mediated by an asymmetric interface. *J. Bacteriol.* 185:254-61

14. Birck C, Mourey L, Gouet P, Fabry B, Schumacher J, et al. 1999. Conformational changes induced by phosphorylation of the FixJ receiver domain. *Structure* 7:1505-15

15. Blanco AG, Sola M, Gomis-Ruth FX, Coll M. 2002. Tandem DNA recognition by PhoB, a two-component signal transduction transcriptional activator. *Structure* 10:701-13

16. Boudes M, Sanchez D, Graille M, van Tilbeurgh H, Durand D, Quevillon-Cheruel S. 2014. Structural insights into the dimerization of the response regulator ComE from *Streptococcus pneumoniae*. *Nucleic Acids Res.* 42:5302-13

17. Bourret RB. 2010. Receiver domain structure and function in response regulator proteins. *Curr. Opin. Microbiol.* 13:142-49

PeerJ Preprints | https://doi.org/10.7287/peerj.preprints.27554v2 | CC BY 4.0 Open Access | rec: 21 Mar 2019, publ: 21 Mar 2019

18. Burley SK, Berman HM, Kleywegt GJ, Markley JL, Nakamura H, Velankar S. 2017. Protein Data Bank (PDB): The single global macromolecular structure archive. *Methods Mol. Biol.* 1607:627-41

19. Capra EJ, Perchuk BS, Skerker JM, Laub MT. 2012. Adaptive mutations that prevent crosstalk enable the expansion of paralogous signaling protein families. *Cell* 150:222-32

20. Casino P, Miguel-Romero L, Huesa J, Garcia P, Garcia-Del Portillo F, Marina A. 2018. Conformational dynamism for DNA interaction in the *Salmonella* RcsB response regulator. *Nucleic Acids Res.* 46:456-72

21. Casino P, Rubio V, Marina A. 2009. Structural insight into partner specificity and phosphoryl transfer in two-component signal transduction. *Cell* 139:325-36

22. Castano-Cerezo S, Bernal V, Post H, Fuhrer T, Cappadona S, et al. 2014. Protein acetylation affects acetate metabolism, motility and acid stress response in *Escherichia coli*. *Mol. Syst. Biol.* 10:762

23. Chakraborty S, Winardhi RS, Morgan LK, Yan J, Kenney LJ. 2017. Non-canonical activation of OmpR drives acid and osmotic stress responses in single bacterial cells. *Nat. Commun.* 8:1587

24. Childers WS, Xu Q, Mann TH, Mathews, II, Blair JA, et al. 2014. Cell fate regulation governed by a repurposed bacterial histidine kinase. *PLoS Biol.* 12:e1001979

25. Cho HS, Lee SY, Yan D, Pan X, Parkinson JS, et al. 2000. NMR structure of activated CheY. *J. Mol. Biol.* 297:543-51

26. Choudhury HG, Beis K. 2013. The dimeric form of the unphosphorylated response regulator BaeR. *Protein Sci.* 22:1287-93

PeerJ Preprints | https://doi.org/10.7287/peerj.preprints.27554v2 | CC BY 4.0 Open Access | rec: 21 Mar 2019, publ: 21 Mar 2019

613 27. Correa F, Gardner KH. 2016. Basis of mutual domain inhibition in a bacterial response
614 regulator. *Cell Chem. Biol.* 23:945-54
615 28. Creager-Allen RL, Silversmith RE, Bourret RB. 2013. A link between dimerization and
616 autophosphorylation of the response regulator PhoB. *J. Biol. Chem.* 288:21755-69
617 29. Davlieva M, Tovar-Yanez A, DeBruler K, Leonard PG, Zianni MR, et al. 2016. An adaptive
618 mutation in *Enterococcus faecium* LiaR associated with antimicrobial peptide resistance
619 mimics phosphorylation and stabilizes LiaR in an activated state. *J. Mol. Biol.* 428:4503-19
620 30. de Been M, Tempelaars MH, van Schaik W, Moezelaar R, Siezen RJ, Abee T. 2010. A novel
621 hybrid kinase is essential for regulating the sigma(B)-mediated stress response of *Bacillus*
622 *cereus*. *Environ. Microbiol.* 12:730-45
623 31. Djordjevic S, Goudreau PN, Xu Q, Stock AM, West AH. 1998. Structural basis for
624 methylesterase CheB regulation by a phosphorylation-activated domain. *Proc. Natl. Acad. Sci.*
625 *USA* 95:1381-86
626 32. Doucleff M, Chen B, Maris AE, Wemmer DE, Kondrashkina E, Nixon BT. 2005. Negative
627 regulation of AAA+ ATPase assembly by two component receiver domains: a transcription
628 activation mechanism that is conserved in mesophilic and extremely hyperthermophilic
629 bacteria. *J. Mol. Biol.* 353:242-55
630 33. Dubey BN, Lori C, Ozaki S, Fucile G, Plaza-Menacho I, et al. 2016. Cyclic di-GMP mediates a
631 histidine kinase/phosphatase switch by noncovalent domain cross-linking. *Sci. Adv.*
632 2:e1600823
633 34. Dutta R, Inouye M. 1996. Reverse phosphotransfer from OmpR to EnvZ in a kinase$^-$
634 /phosphatase$^+$ mutant of EnvZ (EnvZ$^-$N347D), a bifunctional signal transducer of *Escherichia*
635 *coli*. *J. Biol. Chem.* 271:1424-29

PeerJ Preprints | https://doi.org/10.7287/peerj.preprints.27554v2 | CC BY 4.0 Open Access | rec: 21 Mar 2019, publ: 21 Mar 2019

35. El-Gebali S, Mistry J, Bateman A, Eddy SR, Luciani A, et al. 2018. The Pfam protein families database in 2019. *Nucleic Acids Res.*:[Epub ahead of print]

36. Fernandez I, Cornaciu I, Carrica MD, Uchikawa E, Hoffmann G, et al. 2017. Three-dimensional structure of full-length NtrX, an unusual member of the NtrC family of response regulators. *J. Mol. Biol.* 429:1192-212

37. Fernandez I, Otero LH, Klinke S, Carrica MDC, Goldbaum FA. 2015. Snapshots of conformational changes shed light into the NtrX receiver domain signal transduction mechanism. *J. Mol. Biol.* 427:3258-72

38. Filippova EV, Zemaitaitis B, Aung T, Wolfe AJ, Anderson WF. 2018. Structural basis for DNA recognition by the two-component response regulator RcsB. *MBio* 9:01993-17

39. Fraiberg M, Afanzar O, Cassidy CK, Gabashvili A, Schulten K, et al. 2015. CheY's acetylation sites responsible for generating clockwise flagellar rotation in *Escherichia coli*. *Mol. Microbiol.* 95:231-44

40. Friedland N, Mack TR, Yu M, Hung L-W, Terwilliger TC, et al. 2007. Domain orientation in the inactive response regulator *Mycobacterium tuberculosis* MtrA provides a barrier to activation. *Biochemistry* 46:6733-43

41. Galperin MY, Makarova KS, Wolf YI, Koonin EV. 2018. Phyletic distribution and lineage-specific domain architectures of archaeal two-component signal transduction systems. *J. Bacteriol.* 200:e00681-17

42. Gao R, Stock AM. 2010. Molecular strategies for phosphorylation-mediated regulation of response regulator activity. *Curr. Opin. Microbiol.* 13:160-67

43. Gao R, Stock AM. 2017. Quantitative kinetic analyses of shutting off a two-component system. *MBio* 8:e00412-17

PeerJ Preprints | https://doi.org/10.7287/peerj.preprints.27554v2 | CC BY 4.0 Open Access | rec: 21 Mar 2019, publ: 21 Mar 2019

659 44. Gardino AK, Villali J, Kivenson A, Lei M, Liu CF, et al. 2009. Transient non-native hydrogen
660 bonds promote activation of a signaling protein. *Cell* 139:1109-18
661 45. Gottschlich L, Bortfeld-Miller M, Gabelein C, Dintner S, Vorholt JA. 2018. Phosphorelay
662 through the bifunctional phosphotransferase PhyT controls the general stress response in an
663 alphaproteobacterium. *PLoS Genet.* 14:e1007294
664 46. Grimshaw CE, Huang S, Hanstein CG, Strauch MA, Burbulys D, et al. 1998. Synergistic
665 kinetic interactions between components of the phosphorelay controlling sporulation in
666 *Bacillus subtilis*. *Biochemistry* 37:1365-75
667 47. Hastings CA, Lee SY, Cho HS, Yan D, Kustu S, Wemmer DE. 2003. High-resolution solution
668 structure of the beryllofluoride-activated NtrC receiver domain. *Biochemistry* 42:9081-90
669 48. He X, Wang L, Wang S. 2016. Structural basis of DNA sequence recognition by the response
670 regulator PhoP in *Mycobacterium tuberculosis*. *Sci Rep* 6:24442
671 49. Hentchel KL, Escalante-Semerena JC. 2015. Acylation of biomolecules in prokaryotes: a
672 widespread strategy for the control of biological function and metabolic stress. *Microbiol. Mol.*
673 *Biol. Rev.* 79:321-46
674 50. Hong E, Lee HM, Ko H, Kim DU, Jeon BY, et al. 2007. Structure of an atypical orphan
675 response regulator protein supports a new phosphorylation-independent regulatory mechanism.
676 *J. Biol. Chem.* 282:20667-75
677 51. Hu LI, Chi BK, Kuhn ML, Filippova EV, Walker-Peddakotla AJ, et al. 2013. Acetylation of
678 the response regulator RcsB controls transcription from a small RNA promoter. *J. Bacteriol.*
679 195:4174-86
680 52. Huynh TN, Stewart V. 2011. Negative control in two-component signal transduction by
681 transmitter phosphatase activity. *Mol. Microbiol.* 82:275-86

PeerJ Preprints | https://doi.org/10.7287/peerj.preprints.27554v2 | CC BY 4.0 Open Access | rec: 21 Mar 2019, publ: 21 Mar 2019

682 53. Immormino RM, Silversmith RE, Bourret RB. 2016. A variable active site residue influences
683 the kinetics of response regulator phosphorylation and dephosphorylation. *Biochemistry*
684 55:5595-609
685 54. Inclan YF, Laurent S, Zusman DR. 2008. The receiver domain of FrzE, a CheA-CheY fusion
686 protein, regulates the CheA histidine kinase activity and downstream signalling to the A- and
687 S-motility systems of *Myxococcus xanthus*. *Mol. Microbiol.* 68:1328-39
688 55. King-Scott J, Nowak E, Mylonas E, Panjikar S, Roessle M, et al. 2007. The structure of a full-
689 length response regulator from *Mycobacterium tuberculosis* in a stabilized three-dimensional
690 domain-swapped, activated state. *J. Biol. Chem.* 282:37717-29
691 56. Lau J, Hernandez-Alicea L, Vass RH, Chien P. 2015. A phosphosignaling adaptor primes the
692 AAA+ protease ClpXP to drive cell cycle-regulated proteolysis. *Mol. Cell* 59:104-16
693 57. Laub MT, Goulian M. 2007. Specificity in two-component signal transduction pathways. *Annu.*
694 *Rev. Genet.* 41:121-45
695 58. Lee SY, De La Torre A, Yan D, Kustu S, Nixon BT, Wemmer DE. 2003. Regulation of the
696 transcriptional activator NtrC1: structural studies of the regulatory and AAA^+ ATPase domains.
697 *Genes Dev.* 17:2552-63
698 59. Lehman MK, Bose JL, Sharma-Kuinkel BK, Moormeier DE, Endres JL, et al. 2015.
699 Identification of the amino acids essential for LytSR-mediated signal transduction in
700 *Staphylococcus aureus* and their roles in biofilm-specific gene expression. *Mol. Microbiol.*
701 95:723-37
702 60. Leonard PG, Golemi-Kotra D, Stock AM. 2013. Phosphorylation-dependent conformational
703 changes and domain rearrangements in *Staphylococcus aureus* VraR activation. *Proc. Natl.*
704 *Acad. Sci. USA* 110:8525-30

PeerJ Preprints | https://doi.org/10.7287/peerj.preprints.27554v2 | CC BY 4.0 Open Access | rec: 21 Mar 2019, publ: 21 Mar 2019

705 61. Lin W, Wang Y, Han X, Zhang Z, Wang C, et al. 2014. Atypical OmpR/PhoB subfamily
706 response regulator GlnR of actinomycetes functions as a homodimer, stabilized by the
707 unphosphorylated conserved Asp-focused charge interactions. *J. Biol. Chem.* 289:15413-25
708 62. Liu Y, Rose J, Huang S, Hu Y, Wu Q, et al. 2017. A pH-gated conformational switch regulates
709 the phosphatase activity of bifunctional HisKA-family histidine kinases. *Nat. Commun.* 8:2104
710 63. Lori C, Kaczmarczyk A, de Jong I, Jenal U. 2018. A single-domain response regulator
711 functions as an integrating hub to coordinate general stress response and development in
712 alphaproteobacteria. *MBio* 9:e00809-18
713 64. Lou YC, Wang I, Rajasekaran M, Kao YF, Ho MR, et al. 2014. Solution structure and tandem
714 DNA recognition of the C-terminal effector domain of PmrA from *Klebsiella pneumoniae*.
715 *Nucleic Acids Res.* 42:4080-93
716 65. Lou YC, Weng TH, Li YC, Kao YF, Lin WF, et al. 2015. Structure and dynamics of
717 polymyxin-resistance-associated response regulator PmrA in complex with promoter DNA.
718 *Nat. Commun.* 6:8838
719 66. Luebke JL, Eaton DS, Sachleben JR, Crosson S. 2018. Allosteric control of a bacterial stress
720 response system by an anti-sigma factor. *Mol. Microbiol.* 107:164-79
721 67. Lukat GS, McCleary WR, Stock AM, Stock JB. 1992. Phosphorylation of bacterial response
722 regulator proteins by low molecular weight phospho-donors. *Proc. Natl. Acad. Sci. USA*
723 89:718-22
724 68. Martinez-Hackert E, Stock AM. 1997. Structural relationships in the OmpR family of winged-
725 helix transcription factors. *J. Mol. Biol.* 269:301-12
726 69. Mascher T, Helmann JD, Unden G. 2006. Stimulus perception in bacterial signal-transducing
727 histidine kinases. *Microbiol. Mol. Biol. Rev.* 70:910-38

PeerJ Preprints | https://doi.org/10.7287/peerj.preprints.27554v2 | CC BY 4.0 Open Access | rec: 21 Mar 2019, publ: 21 Mar 2019

728 70. McDonald LR, Boyer JA, Lee AL. 2012. Segmental motions, not a two-state concerted switch,
729 underlie allostery in CheY. *Structure* 20:1363-73
730 71. Mechaly AE, Haouz A, Sassoon N, Buschiazzo A, Betton JM, Alzari PM. 2018.
731 Conformational plasticity of the response regulator CpxR, a key player in
732 Gammaproteobacteria virulence and drug-resistance. *J. Struct. Biol.* 204:165-71
733 72. Mechaly AE, Soto Diaz S, Sassoon N, Buschiazzo A, Betton JM, Alzari PM. 2017. Structural
734 coupling between autokinase and phosphotransferase reactions in a bacterial histidine kinase.
735 *Structure* 25:939-44.e3
736 73. Milani M, Leoni L, Rampioni G, Zennaro E, Ascenzi P, Bolognesi M. 2005. An active-like
737 structure in the unphosphorylated StyR response regulator suggests a phosphorylation-
738 dependent allosteric activation mechanism. *Structure* 13:1289-97
739 74. Mo G, Zhou H, Kawamura T, Dahlquist FW. 2012. Solution structure of a complex of the
740 histidine autokinase CheA with its substrate CheY. *Biochemistry* 51:3786-98
741 75. Müller S, Pflock M, Schär J, Kennard S, Beier D. 2007. Regulation of expression of atypical
742 orphan response regulators of *Helicobacter pylori*. *Microbiol. Res.* 162:1-14
743 76. Narayanan A, Paul LN, Tomar S, Patil DN, Kumar P, Yernool DA. 2012. Structure-function
744 studies of DNA binding domain of response regulator KdpE reveals equal affinity interactions
745 at DNA half-sites. *PLoS One* 7:e30102
746 77. Nesper J, Hug I, Kato S, Hee CS, Habazettl JM, et al. 2017. Cyclic di-GMP differentially tunes
747 a bacterial flagellar motor through a novel class of CheY-like regulators. *Elife* 6
748 78. Nowak E, Panjikar S, Konarev P, Svergun DI, Tucker PA. 2006. The structural basis of signal
749 transduction for the response regulator PrrA from *Mycobacterium tuberculosis*. *J. Biol. Chem.*
750 281:9659-66

PeerJ Preprints | https://doi.org/10.7287/peerj.preprints.27554v2 | CC BY 4.0 Open Access | rec: 21 Mar 2019, publ: 21 Mar 2019

79. O'Hara BP, Norman RA, Wan PT, Roe SM, Barrett TE, et al. 1999. Crystal structure and induction mechanism of AmiC-AmiR: a ligand-regulated transcription antitermination complex. *EMBO J.* 18:5175-86

80. Page SC, Immormino RM, Miller TH, Bourret RB. 2016. Experimental analysis of functional variation within protein families: receiver domain autodephosphorylation kinetics. *J. Bacteriol.* 198:2483-93

81. Parashar V, Mirouze N, Dubnau DA, Neiditch MB. 2011. Structural basis of response regulator dephosphorylation by Rap phosphatases. *PLoS Biol.* 9:e1000589

82. Park AK, Lee JH, Chi YM, Park H. 2016. Structural characterization of the full-length response regulator spr1814 in complex with a phosphate analogue reveals a novel conformational plasticity of the linker region. *Biochem. Biophys. Res. Commun.* 473:625-9

83. Park AK, Moon JH, Lee KS, Chi YM. 2012. Crystal structure of receiver domain of putative NarL family response regulator spr1814 from *Streptococcus pneumoniae* in the absence and presence of the phosphoryl analog beryllofluoride. *Biochem. Biophys. Res. Commun.* 421:403-7

84. Park S, Meyer M, Jones AD, Yennawar HP, Yennawar NH, Nixon BT. 2002. Two-component signaling in the AAA^+ ATPase DctD: binding Mg^{2+} and BeF_3^- selects between alternate dimeric states of the receiver domain. *FASEB J.* 16:1964-66

85. Patel K, Golemi-Kotra D. 2015. Signaling mechanism by the *Staphylococcus aureus* two-component system LytSR: role of acetyl phosphate in bypassing the cell membrane electrical potential sensor LytS. *F1000Res.* 4:79

PeerJ Preprints | https://doi.org/10.7287/peerj.preprints.27554v2 | CC BY 4.0 Open Access | rec: 21 Mar 2019, publ: 21 Mar 2019

772 86. Pazy Y, Motaleb MA, Guarnieri MT, Charon NW, Zhao R, Silversmith RE. 2010. Identical
773 phosphatase mechanisms achieved through distinct modes of binding phosphoprotein substrate.
774 *Proc. Natl. Acad. Sci. USA* 107:1924-29
775 87. Pazy Y, Wollish AC, Thomas SA, Miller PJ, Collins EJ, et al. 2009. Matching biochemical
776 reaction kinetics to the timescales of life: structural determinants that influence the
777 autodephosphorylation rate of response regulator proteins. *J. Mol. Biol.* 392:1205-20
778 88. Podgornaia AI, Laub MT. 2013. Determinants of specificity in two-component signal
779 transduction. *Curr. Opin. Microbiol.* 16:156-62
780 89. Pontiggia F, Pachov DV, Clarkson MW, Villali J, Hagan MF, et al. 2015. Free energy
781 landscape of activation in a signalling protein at atomic resolution. *Nat. Commun.* 6:7284
782 90. Ramakrishnan R, Schuster M, Bourret RB. 1998. Acetylation at Lys-92 enhances signaling by
783 the chemotaxis response regulator protein CheY. *Proc. Natl. Acad. Sci. USA* 95:4918-23
784 91. Robinson VL, Wu T, Stock AM. 2003. Structural analysis of the domain interface in DrrB, a
785 response regulator of the OmpR/PhoB subfamily. *J. Bacteriol.* 185:4186-94
786 92. Romling U, Gomelsky M, Galperin MY. 2005. C-di-GMP: the dawning of a novel bacterial
787 signalling system. *Mol. Microbiol.* 57:629-39
788 93. Ruiz D, Salinas P, Lopez-Redondo ML, Cayuela ML, Marina A, Contreras A. 2008.
789 Phosphorylation-independent activation of the atypical response regulator NblR. *Microbiology*
790 154:3002-15
791 94. Sidote DJ, Barbieri CM, Wu T, Stock AM. 2008. Structure of the *Staphylococcus aureus* AgrA
792 LytTR domain bound to DNA reveals a beta fold with an unusual mode of binding. *Structure*
793 16:727-35

PeerJ Preprints | https://doi.org/10.7287/peerj.preprints.27554v2 | CC BY 4.0 Open Access | rec: 21 Mar 2019, publ: 21 Mar 2019

794 95. Simonovic M, Volz K. 2001. A distinct meta-active conformation in the 1.1-Å resolution
795 structure of wild-type apoCheY. *J. Biol. Chem.* 276:28637-40
796 96. Skerker JM, Perchuk BS, Siryaporn A, Lubin EA, Ashenberg O, et al. 2008. Rewiring the
797 specificity of two-component signal transduction systems. *Cell* 133:1043-54
798 97. Sourjik V, Schmitt R. 1996. Different roles of CheY1 and CheY2 in the chemotaxis of
799 *Rhizobium meliloti*. *Mol. Microbiol.* 22:427-36
800 98. Sourjik V, Schmitt R. 1998. Phosphotransfer between CheA, CheY1, and CheY2 in the
801 chemotaxis signal transduction chain of *Rhizobium meliloti*. *Biochemistry* 37:2327-35
802 99. Stock AM, Robinson VL, Goudreau PN. 2000. Two-component signal transduction. *Annu. Rev.*
803 *Biochem.* 69:183-215
804 100. Surette MG, Levit M, Liu Y, Lukat G, Ninfa EG, et al. 1996. Dimerization is required for the
805 activity of the protein histidine kinase CheA that mediates signal transduction in bacterial
806 chemotaxis. *J. Biol. Chem.* 271:939-45
807 101. Thomas SA, Brewster JA, Bourret RB. 2008. Two variable active site residues modulate
808 response regulator phosphoryl group stability. *Mol. Microbiol.* 69:453-65
809 102. Thomas SA, Immormino RM, Bourret RB, Silversmith RE. 2013. Nonconserved active site
810 residues modulate CheY autophosphorylation kinetics and phosphodonor preference.
811 *Biochemistry* 52:2262-73
812 103. Tindall MJ, Porter SL, Maini PK, Armitage JP. 2010. Modeling chemotaxis reveals the role of
813 reversed phosphotransfer and a bi-functional kinase-phosphatase. *PLoS Comput. Biol.* 6
814 104. Toro-Roman A, Mack TR, Stock AM. 2005. Structural analysis and solution studies of the
815 activated regulatory domain of the response regulator ArcA: a symmetric dimer mediated by
816 the α4-β5-α5 face. *J. Mol. Biol.* 349:11-26

PeerJ Preprints | https://doi.org/10.7287/peerj.preprints.27554v2 | CC BY 4.0 Open Access | rec: 21 Mar 2019, publ: 21 Mar 2019

817 105. Toro-Roman A, Wu T, Stock AM. 2005. A common dimerization interface in bacterial
818 response regulators KdpE and TorR. *Protein Sci.* 14:3077-388
819 106. Trajtenberg F, Albanesi D, Ruetalo N, Botti H, Mechaly AE, et al. 2014. Allosteric activation
820 of bacterial response regulators: the role of the cognate histidine kinase beyond
821 phosphorylation. *MBio* 5:e02105
822 107. Trajtenberg F, Imelio JA, Machado MR, Larrieux N, Marti MA, et al. 2016. Regulation of
823 signaling directionality revealed by 3D snapshots of a kinase:regulator complex in action. *Elife*
824 5:e21422
825 108. Varughese KI. 2005. Conformational changes of Spo0F along the phosphotransfer pathway. *J.*
826 *Bacteriol.* 187:8221-27
827 109. Villali J, Pontiggia F, Clarkson MW, Hagan MF, Kern D. 2014. Evidence against the "Y-T
828 coupling" mechanism of activation in the response regulator NtrC. *J. Mol. Biol.* 426:1554-67
829 110. Volkman BF, Lipson D, Wemmer DE, Kern D. 2001. Two-state allosteric behavior in a single
830 domain signaling protein. *Science* 291:2429-33
831 111. Volz K. 1993. Structural conservation in the CheY superfamily. *Biochemistry* 32:11741-53
832 112. Wang L, Tian X, Wang J, Yang H, Fan K, et al. 2009. Autoregulation of antibiotic biosynthesis
833 by binding of the end product to an atypical response regulator. *Proc. Natl. Acad. Sci. USA*
834 106:8617-22
835 113. Wheeler TJ, Clements J, Finn RD. 2014. Skylign: a tool for creating informative, interactive
836 logos representing sequence alignments and profile hidden Markov models. *BMC*
837 *Bioinformatics* 15:7

PeerJ Preprints | https://doi.org/10.7287/peerj.preprints.27554v2 | CC BY 4.0 Open Access | rec: 21 Mar 2019, publ: 21 Mar 2019

838 114. Willett JW, Herrou J, Briegel A, Rotskoff G, Crosson S. 2015. Structural asymmetry in a
839 conserved signaling system that regulates division, replication, and virulence of an intracellular
840 pathogen. *Proc .Natl. Acad. Sci. USA* 112:E3709-18
841 115. Wolfe AJ. 2010. Physiologically relevant small phosphodonors link metabolism to signal
842 transduction. *Curr. Opin. Microbiol.* 13:204-9
843 116. Wright GSA, Saeki A, Hikima T, Nishizono Y, Hisano T, et al. 2018. Architecture of the
844 complete oxygen-sensing FixL-FixJ two-component signal transduction system. *Sci. Signal.* 11
845 117. Wu J, Ohta N, Newton A. 1998. An essential, multicomponent signal transduction pathway
846 required for cell cycle regulation in *Caulobacter*. *Proc. Natl. Acad. Sci. USA* 95:1443-48
847 118. Yamada S, Sugimoto H, Kobayashi M, Ohno A, Nakamura H, Shiro Y. 2009. Structure of
848 PAS-linked histidine kinase and the response regulator complex. *Structure* 17:1333-44
849 119. Yan D, Cho HS, Hastings CA, Igo MM, Lee SY, et al. 1999. Beryllofluoride mimics
850 phosphorylation of NtrC and other bacterial response regulators. *Proc. Natl. Acad. Sci. USA*
851 96:14789-94
852 120. Yan J, Barak R, Liarzi O, Shainskaya A, Eisenbach M. 2008. *In vivo* acetylation of CheY, a
853 response regulator in chemotaxis of *Escherichia coli*. *J. Mol. Biol.* 376:1260-71
854 121. Zapf J, Madhusudan M, Grimshaw CE, Hoch JA, Varughese KI, Whiteley JM. 1998. A source
855 of response regulator autophosphatase activity: the critical role of a residue adjacent to the
856 Spo0F autophosphorylation active site. *Biochemistry* 37:7725-32
857 122. Zapf J, Sen U, Madhusudan, Hoch JA, Varughese KI. 2000. A transient interaction between
858 two phosphorelay proteins trapped in a crystal lattice reveals the mechanism of molecular
859 recognition and phosphotransfer in signal transduction. *Structure* 8:851-62

PeerJ Preprints | https://doi.org/10.7287/peerj.preprints.27554v2 | CC BY 4.0 Open Access | rec: 21 Mar 2019, publ: 21 Mar 2019

123. Zhao R, Collins EJ, Bourret RB, Silversmith RE. 2002. Structure and catalytic mechanism of the *E. coli* chemotaxis phosphatase CheZ. *Nat. Struct. Biol.* 9:570-75

124. Zhu X, Rebello J, Matsumura P, Volz K. 1997. Crystal structures of CheY mutants Y106W and T87I/Y106W: CheY activation correlates with movement of residue 106. *J. Biol. Chem.* 272:5000-06

125. Zhu Y, Qin L, Yoshida T, Inouye M. 2000. Phosphatase activity of histidine kinase EnvZ without kinase catalytic domain. *Proc. Natl. Acad. Sci. USA* 97:7808-13

PeerJ Preprints | https://doi.org/10.7287/peerj.preprints.27554v2 | CC BY 4.0 Open Access | rec: 21 Mar 2019, publ: 21 Mar 2019

868

869 **TERMS AND DEFINITIONS**
870

871	AcP	acetyl phosphate
872	BeF_3^-	beryllofluoride
873	CA	catalytic/ATP-binding (domain)
874	DBD	DNA-binding domain
875	DHp	dimerization/histidine phosphotransfer (domain)
876	ECF	extracytoplasmic function
877	HK	histidine kinase
878	HPt	histidine-containing phosphotransfer (domain)
879	PDB	Protein Data Bank
880	REC	receiver (domain of response regulator protein)
881	RR	response regulator protein
882	SDRR	single-domain response regulator
883	TCS	two-component system

884

PeerJ Preprints | https://doi.org/10.7287/peerj.preprints.27554v2 | CC BY 4.0 Open Access | rec: 21 Mar 2019, publ: 21 Mar 2019

885 **FIGURE CAPTIONS**

886 **Figure 1**. Common features of RRs. (***a***) Schematic diagram of the prototypical TCS pathway. (***b***)
887 The conserved $(\beta\alpha)_5$ fold of REC domains. Phosphorylation site residues and the phosphoryl group
888 mimic, beryllofluoride (BeF_3^-), are shown in sticks. (***c***) Sequence conservation of RECs. The
889 profiled hidden Markov model (HMM) for the REC protein family (Pfam PF00072) is shown as
890 sequence logos (113) with the secondary structure elements illustrated. Heights of individual stacked
891 letters at each position correspond to information contents, reflecting the probability of observing the
892 particular amino acids at each position. Phosphorylation site residues (stars), named after the most
893 conserved amino acids (DD, D, T and K), are among the most conserved residues in REC domains.

894

895 **Figure 2**. Classification of RRs by their effector domains. The percentile distribution is indicated for
896 RR effector functional classes and RR subfamilies. RR subfamilies are defined by effector domain
897 folds identified in Pfam. Representative proteins are traditionally used to name the OmpR, NarL and
898 NtrC subfamilies with effector domains named Trans_reg_C, GerE and Sigma54_activa in Pfam.
899 Representative structures of each subfamily are shown with REC domains colored in grey and
900 effector domains in colors (PDB ids: KdpE, 4KNY; RcsB, 5W43; LuxO, 5EP0; AgrA, 3BS1; AmiR,
901 1QO0; WspR, 3BRE; CheB, 1A2O).

902

903 **Figure 3**. Phosphorylation site of the REC domain. The phosphoryl group is positioned by a network
904 of hydrogen bonds (dashed lines) with side chains of the highly conserved residues (orange) as well
905 as backbone atoms of non-conserved residues (light pink). Non-conserved active site residues are
906 labeled by their relative sequence positions to the nearest conserved residues, such as T+1, indicating

PeerJ Preprints | https://doi.org/10.7287/peerj.preprints.27554v2 | CC BY 4.0 Open Access | rec: 21 Mar 2019, publ: 21 Mar 2019

907 one residue C-terminal to the conserved Thr/Ser residue. (***a***) Phosphorylation site of the archetype
908 RR CheY in the active conformation (PDB id: 1FQW) with residues that are differently positioned
909 in the inactive conformation (2CHE) shown in cyan. (***b***) The putative trigonal bipyramidal transition
910 state for both phosphorylation and dephosphorylation. X represents the leaving group of the
911 phosphodonor for phosphorylation or the attacking water for dephosphorylation. (***c***) Surface view of
912 the active site in the phosphatase-REC complex (3HZH).

913

914 **Figure 4**. RR regulatory strategies. (***a***) Distinct inactive and active RR conformations exemplified
915 by full-length RR VraR (PDB ids: 4GVP, 4IF4). BeF_3^- is shown in red spheres. (***b***) Schematic
916 diagrams of RR regulatory mechanisms. Functional sites of effector domains, such as enzyme sites
917 or DNA recognition regions, are shown as pink dots. These sites can be buried or exposed in a wide
918 variety of inactive RR conformations and their activity depends on different interactions between the
919 REC and effector domains. Phosphorylation of the RR can relieve REC domain inhibition, promote
920 effector function or both. Representative RRs that utilize these strategies are indicated.

921

922 **Figure 5**. Phosphorylation-induced conformational changes in the REC domain. RR structures with
923 or without BeF_3^- were aligned using the conserved strands β1, β3, β4, and β5 to compute the average
924 backbone RMSD per residue (***a***, *right*). RMSD values above the median + 2x MAD (median
925 absolute deviation) are considered as significant conformational changes and the corresponding
926 residues are colored blue. Non-REC structural elements are colored cyan. BeF_3^- is shown as red
927 spheres and residues involved in the potential Y-T coupling are shown as green or gray sticks.
928 Representative protein structures shown for the (***a***) Stand-alone, (***b***) OmpR, (***c***) NtrC and (***d***) NarL

PeerJ Preprints | https://doi.org/10.7287/peerj.preprints.27554v2 | CC BY 4.0 Open Access | rec: 21 Mar 2019, publ: 21 Mar 2019

929 RR subfamilies are CheY (1F4V), DrrB (3NNS, 1P2F), NtrC1 (1ZY2, 1NY5) and VraR (4IF4). Y/T
930 residues from the inactive CheY structure (2CHE) are differently positioned from the active
931 structure. For the OmpR, NtrC and NarL subfamilies, two proteins from each subfamily were used
932 for RMSD analyses and both showed similar regions of conformational changes. Substantial changes
933 in α1 are also observed in one protein from the NtrC subfamily (pink).

934

935 **Figure 6**. Structure of the HK-RR complex. Ribbon (***a***) and surface (***b***) views of the HK856-RR468
936 complex (PDB id, 3DGE). Residues that determine the HK-RR interaction specificity (19, 96) are
937 highlighted in light orange and cyan in the HK and RR, respectively. HK-RR contacts also involve
938 other surface regions (grey), including both active sites of the HK (red) and the RR (pink).

PeerJ Preprints | https://doi.org/10.7287/peerj.preprints.27554v2 | CC BY 4.0 Open Access | rec: 21 Mar 2019, publ: 21 Mar 2019

Abstract

Response regulators function as the output components of two-component systems, which couple the sensing of environmental stimuli to adaptive responses. Response regulators typically contain conserved receiver (REC) domains that function as phosphorylation-regulated switches to control the activities of effector domains that elicit output responses. This modular design is extremely versatile, enabling different regulatory strategies tuned to the needs of individual signaling systems. This review summarizes functional features that underlie response regulator function. An abundance of atomic resolution structures and complementary biochemical data have defined the mechanisms for response regulator enzymatic activities, revealed trends in regulatory strategies utilized by response regulators of different subfamilies and provided insights into interactions of response regulators with their cognate histidine kinases. Among the hundreds of thousands of response regulators identified, variations abound. This article provides a framework for understanding structural features that enable function of canonical response regulators and a basis for distinguishing non-canonical configurations.

PeerJ Preprints | https://doi.org/10.7287/peerj.preprints.27554v2 | CC BY 4.0 Open Access | rec: 21 Mar 2019, publ: 21 Mar 2019

1. INTRODUCTION

Two-component systems (TCSs) are the predominant multi-step signaling pathways in bacteria. Two conserved proteins, a histidine protein kinase (HK) and response regulator (RR), constitute the core system (**Figure 1*a***). Autophosphorylation of the HK at a conserved His provides a high-energy phosphoryl group that is transferred to a conserved Asp in the RR, resulting in RR activation (99). Stimuli, sensed either directly or indirectly by the HK, regulate opposing autophosphorylation/phosphotransfer and RR phosphatase activities of the HK, thus determining the level of phosphorylation of the RR and the output response. A large variety of input domains in HKs and output domains in RRs allows the coupling of an almost limitless array of chemical or physical stimuli to diverse output responses. The conserved proteins and the systems themselves are extremely versatile. An enormous range of variations in protein activities, domain architectures and system configurations allows adaptation of TCSs to the needs of specific signaling systems.

TCSs are found in bacteria, archaea (41) and eukaryotes such as slime molds, yeast, and plants (2). While great diversity exists among all TCSs it should be noted that some specific trends in system configurations are found in different organisms. The Pfam database (35) lists >342,000 entries of proteins containing the conserved receiver (REC, named Response_reg in Pfam) domain that characterizes RRs and >650 structures of such proteins in the Protein Data Bank (PDB) (18). In addition to their presence in RRs, REC domains are also found in hybrid HKs that function within phospho-relay systems involving multiple phosphotransfer steps, accounting for ~10% of REC domain-containing proteins. The scope of this review will focus on bacterial RRs that mediate output of TCSs. Among these RRs, variations abound. The plasticity of the REC domain and the versatility of TCS architecture has driven the evolution of RRs that

PeerJ Preprints | https://doi.org/10.7287/peerj.preprints.27554v2 | CC BY 4.0 Open Access | rec: 21 Mar 2019, publ: 21 Mar 2019

are uniquely adapted and fine-tuned for function in specific pathways. Out of necessity, this review will focus on canonical RRs with full understanding, but lack of specific acknowledgement of individual cases, that for every feature noted, exceptions exist.

This review provides an overview of the structure of RRs and features that provide conserved enzymatic activities in REC domains. Beyond the core domain structures and common enzymatic mechanisms, RRs display great variation in domain arrangements that provide a variety of mechanistically distinct regulatory mechanisms. However, as structures have accumulated, trends in regulatory strategies used by different subfamilies of RRs have begun to emerge and these will be explored in this review.

2. RESPONSE REGULATOR ARCHITECTURE

REC Domains

RRs are defined by the presence of a conserved REC domain. The REC domain fold is composed of five α helices surrounding a central five-stranded parallel β-sheet with a 21345 topology (**Figure 1*b***). Sequence identity between REC domains is usually 20-30%, showing great variations (**Figure 1*c***). The central hydrophobic β-strands, β1, β3, β4 and β5, are more conserved than the peripheral helices and loops. The most conserved residues include the site of phosphorylation, an Asp at the *C*-terminus of β3, and several other residues in the β-α loops, which constitute the active site. The highly conserved phosphorylation site and the variable peripheral sequences allow RRs to couple phosphorylation to diverse effector functions.

Effector Domains

RRs typically function as the output components of signaling pathways. Regulatory REC domains can be linked either covalently or non-covalently to a great diversity of effectors and

PeerJ Preprints | https://doi.org/10.7287/peerj.preprints.27554v2 | CC BY 4.0 Open Access | rec: 21 Mar 2019, publ: 21 Mar 2019

thus control numerous diverse responses. **Figure 2** summarizes the distribution of the major RR effector domains identified in the Pfam database. Approximately one fourth of RRs (23%) consist solely of a REC domain. These single-domain RRs (SDRRs) regulate intermolecular effectors such as the chemotaxis system regulator CheY, which binds to the flagellar motor component FliM controlling flagellar rotation. CheY-like proteins found in chemotaxis-like or chemosensory systems mediate responses other than chemotaxis, for example biofilm formation regulated by Cle proteins (77). Other functions for SDRRs include acting as intermediates in phosphorelays (e.g. the general stress response proteins SdrG and MrrA, and the sporulation protein Spo0F) (45, 63), as phosphate sinks to control phosphate flux within phosphorelays (e.g. *Rhizobium meliloti* CheY1) (97), as allosteric regulators of HKs (e.g. *Caulobacter crescentus* DivK) (24, 117) or as protease adapters (e.g. *C. crescentus* CpdR) (56).

The largest class of RRs (64.5%) is composed of RRs containing a DNA-binding domain (DBD) with subfamilies defined by different DBD folds. The OmpR subfamily (29% of RRs) contains a winged-helix effector domain (68), the NarL subfamily (19%) a four-helix DNA-binding HTH domain (73), the NtrC subfamily (7%) a Fis-type HTH domain fused to an AAA+ ATPase domain and the LytTR (5.5%) a predominantly β fold (94). The abundance of RRs in this class likely reflects the importance of transcriptional regulation as a response to environmental change. A small class of RRs (1%) harbors an RNA-binding domain belonging to the ANTAR subfamily of anti-termination factors such as AmiR (79).

RRs with enzymatic domains account for ~8% of RRs. A major group within this class (3% of RRs) is the regulators of cyclic di-GMP including cyclases (GGDEF) and phosphodiesterases (EAL, HD-GYP) (92). A second major group (2%) is the chemotaxis methylesterase CheB proteins (31). A variety of different enzymatic domains have been identified in other RRs (3%)

PeerJ Preprints | https://doi.org/10.7287/peerj.preprints.27554v2 | CC BY 4.0 Open Access | rec: 21 Mar 2019, publ: 21 Mar 2019

such as the PP2C phosphatase domain of RsbY and the hybrid kinase domain of FrzE (30, 54). RRs with protein binding domains account for ~1% of RRs. Examples in this class include CheV, with a CheW-like domain that connects chemoreceptors to the chemotaxis histidine kinase CheA; RssB, which regulates turnover of the stress response sigma factor RpoS; and PhyR, a regulator of the general stress response that contains an extracytoplasmic function (ECF) sigma factor-like domain (1, 11, 66). While RRs often contain a simple REC-effector domain architecture they can have complex domain organizations with additional signaling domains including PAS, GAF, HisKa, HATPase, etc. The large variety of RRs identified to date emphasizes the versatility of the REC domain with no apparent limits on the types of effector domains that can be controlled by this phosphorylation-activated switch.

3. ENZYMATIC ACTIVITIES OF RRs

Conserved Phosphorylation Site

One of the defining characteristics of the REC domain is its highly conserved phosphorylation site. Due to the lability of the high-energy acyl phosphate, structural characterization of the active site often relies on beryllofluoride (BeF_3^-) that noncovalently binds to the phosphorylation site Asp and serves as a mimic of the phosphoryl group (119). Different BeF_3^--bound RR structures reveal a conserved active site with a network of hydrogen bonds (**Figure 3*a***). The carboxylate side chains of the acidic residue duo (DD) at the β1-α1 loop participate in coordinating a Mg^{2+} required for catalysis. Sidechains of two additional residues, a Thr/Ser (T) at the β4-α4 loop and a Lys (K) at the β5-α5 loop, together with backbone atoms of non-conserved active site residues, coordinate phosphate oxygens in the phosphorylated REC domain.

PeerJ Preprints | https://doi.org/10.7287/peerj.preprints.27554v2 | CC BY 4.0 Open Access | rec: 21 Mar 2019, publ: 21 Mar 2019

RR phosphorylation level, the ultimate determining factor of TCS output for canonical RRs, is regulated by multiple enzyme activities, including phosphotransfer from HKs, dephosphorylation by auxiliary phosphatases or bifunctional HKs that also possess RR phosphatase activity, autophosphorylation by small-molecule phosphodonors such as phosphoramidate and acetyl phosphate (AcP) (67, 115), and autodephosphorylation activities. Similar phosphorylation sites with almost identical positioning of active site residues have been observed in numerous RR or RR complex structures (21, 81, 86, 107). A pentavalent phosphorus intermediate is believed to be a common transition state for different activities of the REC domain (**Figure 3*b***). Both phosphorylation and dephosphorylation reactions can proceed through either an associative or a dissociative mechanism depending on how tight or extended the transition state is. A phosphodonor or water molecule needs to be in line with the acyl phosphate bond that is to be formed or broken. The phosphotransferase or phosphatase helps position these molecules to further enhance the reaction rates. In all cases, the majority of residues involved in coordinating the phosphorus intermediate are from the REC domain. Thus, most RRs are catalytically competent of autophosphorylation and autodephosphorylation in the absence of any enzymatic protein partner and in vitro analyses of these reactions often provide insights into RR regulatory mechanisms.

Autodephosphorylation and Autophosphorylation

Despite the highly conserved active site geometry, RRs show large variations in rates of autophosphorylation and autodephosphorylation (87, 101, 102). For example, autodephosphorylation rate constants of the REC domain range over six orders of magnitude, giving phosphorylation half-lives of seconds to hours and even days (101). Such great diversity is partly attributed to several variable residues surrounding the active site, such as positions D+2

PeerJ Preprints | https://doi.org/10.7287/peerj.preprints.27554v2 | CC BY 4.0 Open Access | rec: 21 Mar 2019, publ: 21 Mar 2019

(two residues *C*-terminal to the conserved D), T+1 and T+2 (one and two residues *C*-terminal to T) (**Figure 3*b* and 3*c***). Backbone atoms of D+2 and T+1 directly form hydrogen bonds with the phosphoryl group while the charge, size and hydrophobicity of sidechains at these three positions may affect the energy barrier of the transition state, facilitate the positioning or block the in-line path of the phosphodonor or attacking water (53, 80, 102, 121). In more than half of RR sequences, a limited number of amino acid combinations are preferred at these positions and the distribution of preferred amino acids correlates with RR effector subfamilies (53, 80). REC enzyme activities are therefore suggested to co-evolve with effector domain regulation and these residues represent functional sites for modulating the stability of RR phosphorylation to match the timescale of individual TCS output responses.

Phosphorylation by small molecules, particularly AcP, has long been suggested to be physiologically relevant in some RRs to couple TCS output to global conditions (115). RR phosphorylation, often in the absence of the cognate HK, can be influenced by cellular AcP levels that are sensitive to the metabolic state of cell. Because the phosphorylation rate by AcP is usually much slower than the rate of phosphotransfer by the cognate HK and often offset by the phosphatase activity of bifunctional HKs or other auxiliary phosphatases (43, 57), the contribution of phosphorylation by AcP to TCS output is typically minimal in wild-type cells. However, given the great diversity of TCSs, AcP can play a significant role in some systems, specifically those with a fast RR autophosphorylation rate and/or a slow phosphatase rate (59, 85).

HK-mediated Activities

RR phosphatase activities mediated by HKs or auxiliary phosphatases are believed to function through positioning a water molecule and stimulating the intrinsic RR autophosphatase activity

PeerJ Preprints | https://doi.org/10.7287/peerj.preprints.27554v2 | CC BY 4.0 Open Access | rec: 21 Mar 2019, publ: 21 Mar 2019

(17). Structure of CheY3 complexed with the phosphatase CheX (86) reveals an amide side chain inserting into the RR active site and forming a hydrogen bond with the attacking water molecule (**Figure 3*c***). Similar positioning of the amide from a Gln or Asn residue has been observed in different phosphatases with distinct structures, such as CheX (86), CheZ (123) and RapH (81), as well as the phosphatase state of DesK, a bifunctional HK from the second largest HK subfamily, HisKA_3 (107). The Gln-containing sequence motif, DXXXQ, is located immediately after the phospho-accepting His residue in HKs from the HisKA_3 subfamily. The His residue does not appear to be required for RR dephosphorylation despite its close proximity to the phosphatase-essential Gln (52) . For the largest HK subfamily, HisKA, the His residue may play a role in RR dephosphorylation (62, 125) but the exact phosphatase mechanism is less clear. An EXXN/T motif similar to CheX-like phosphatases has been identified and the conserved Asn/Thr residue is suggested to be the catalytic residue (52). However, among the available structures of RR complexes with HKs of the HisKA subfamily, the side chain of the Asn/Thr residue is not at a similar position as the Asn/Gln in other phosphatases and is distant from the active site Asp. A dual engagement model has been suggested involving both His and Asn/Thr residues positioning the catalytic water molecule (62). Roles of the two residues may differ for individual HisKA proteins depending on structural details and structures unequivocally capturing the phosphatase state are needed to elucidate the mechanism.

Loss of RR phosphorylation can result from autodephosphorylation, dephosphorylation by the HK and back-transfer to the cognate HK (34, 98), i.e. the reverse reaction of phosphotransfer. The back-transferred histidyl phosphoryl group can be further transferred to ADP (46, 100) or to other RRs that function as phosphate sinks to modulate phosphorylation levels (3, 98, 103). Back-transfer is suggested to accompany an associative transfer mechanism

PeerJ Preprints | https://doi.org/10.7287/peerj.preprints.27554v2 | CC BY 4.0 Open Access | rec: 21 Mar 2019, publ: 21 Mar 2019

that has a tight RR phosphorylation transition state and appears to be evolved for bi-directional transfer common in CheA or other HPt-containing phosphorelay proteins (107, 122). Unidirectional phosphotransfer with little back-transfer, observed in several canonical HKs, is linked to a dissociative mechanism and the asymmetry of the Mg^{2+} position in an extended transition state (107). The dissociative mechanism can be distinguished by a long distance between the conserved Asp and His residues in an HK-RR complex structure. It remains to be investigated whether there is any domain preference or sequence signature that distinguishes the two mechanisms and determines the relative rates of forward- and back-transfer. Residues affecting the transition state stability, such as non-conserved residues at D+2, T+1 and T+2 positions, also modulate the HK-catalyzed phosphotransfer rate (53, 107). Due to multiple phosphorylation and dephosphorylation reactions present simultaneously, quantitation of individual activities is often complicated by interference from other activities. Furthermore, RR activities measured *in vitro* with truncated cytoplasmic fragments of transmembrane HKs require careful examination and may differ greatly from their full-length counterparts in the cellular environment (43).

4. REGULATORY MECHANISMS IN RR SUBFAMILIES

As a phosphorylation-activated switch between inactive and active conformations, the REC domain mediates effector functions through intramolecular and/or intermolecular interactions. Structures of individual REC and effector domains usually undergo subtle changes upon phosphorylation, but the overall structures may vary greatly because of different domain arrangements. A typical RR regulatory mechanism is exemplified by *Staphylococcus aureus* VraR (**Figure 4*a*)**, one of a few RRs with full-length protein structures available in both

PeerJ Preprints | https://doi.org/10.7287/peerj.preprints.27554v2 | CC BY 4.0 Open Access | rec: 21 Mar 2019, publ: 21 Mar 2019

phosphorylated (or BeF_3^--bound) and unphosphorylated states (60). The monomeric unphosphorylated VraR adopts a closed conformation with extensive contacts between the REC and DBD effector domains, holding the DNA-recognition helix at a position unfavorable for dimerization on DNA. Phosphorylation results in an extended conformation with a flexible linker between the two domains and an altered REC surface that promotes RR dimerization for DNA binding.

Negative regulation in the inactive state and positive regulation in the active state, as shown for VraR, are two common mechanisms mediated by the REC domain (**Figure 4*b***). For positive regulation, the REC domain facilitates the effector domain function, as shown for many DBD-containing RRs in which dimerization of the phosphorylated REC domains is thought to promote DNA binding and transcription regulation. Effector domains of some RRs, such as NtrC1 (58) and CheB (31), are catalytically competent when alone, but are inhibited by the REC domain in the inactive state. The two mechanisms are not exclusive and many RRs use both. Regulatory details for individual RRs show great variations that may have been evolved to adapt each protein to its unique structure and function. For example, in inactive states, interactions between REC and effector domains can differ dramatically (**Figure 4*b***), even within the same subfamily of RRs (42). Functional sites, such as the DNA-recognition helix for DBDs and the active site for enzymatic effector domains, can be buried within the REC-effector interface or exposed but held at unfavorable positions by tight interactions. Extended conformations with few interdomain contacts have also been observed for a few RRs that are believed to employ a positive regulatory mechanism.

Inactive and Active Conformational States

PeerJ Preprints | https://doi.org/10.7287/peerj.preprints.27554v2 | CC BY 4.0 Open Access | rec: 21 Mar 2019, publ: 21 Mar 2019

The REC interaction surface that mediates effector domain function is usually distant from the phosphorylation site. A dynamic allosteric mechanism allows conformational changes at the phosphorylation site to propagate to the distal interaction surface. The REC domain samples different allosteric conformations and exists in equilibrium between inactive and active conformations, with phosphorylation shifting the equilibrium. A "Y-T coupling" allosteric mechanism was initially described for CheY (25, 124) and several other RRs (14, 47). Rearrangement of the conserved T at the phosphorylation site (**Figure 3*a***) is believed to correlate with the rotameric conformation of a conserved Tyr/Phe (Y) residue in the β5 strand. In the active state, the aromatic side chain is oriented toward the interior of the REC domain, distinct from the outward position in the inactive state (**Figure 5*a***), resulting in alteration of the α4-β5-α5 face, a surface widely used by many RRs for interdomain interactions. Because of the readily recognizable position of the two residues, they are often used to classify structures as inactive or active, with the caveat that the conformational change involves a broad surface of the REC domain and Y-T coupling is not the only allosteric mechanism (20, 109).

X-ray crystallography has been central to understanding RR regulatory mechanisms although conformations trapped in crystals represent only static snapshots of RR conformational dynamics and can be influenced by experimental conditions, crystal lattice contacts and high protein concentrations used in crystallization. A particular interaction interface or dimerization/oligomerization mode observed in crystal structures, such as domain-swapped dimers observed in several RRs (17, 26, 55), may not be physiologically relevant and requires complementary experiments for validation. Nevertheless, an increasing number of RR structure snapshots start to reveal different states of conformational trajectories and trends of prevalent regulatory strategies in RR subfamilies.

PeerJ Preprints | https://doi.org/10.7287/peerj.preprints.27554v2 | CC BY 4.0 Open Access | rec: 21 Mar 2019, publ: 21 Mar 2019

DBD-containing RRs, the largest class of RRs, have the greatest number of X-ray structures available, making it possible to analyze the allosteric conformational features within individual RR subfamilies (**Table 1**). All structures crystalized with phosphorylated or BeF_3^--bound RRs display inward orientations of the side chain at the conserved Y position while conformations of unphosphorylated RRs are diverse. For unphosphorylated RRs in the OmpR and NtrC subfamilies, both outward and inward orientations of Y residues have been observed, with the inward orientation more readily observed for the REC domain alone than for multi-domain proteins (**Table 1**). This is consistent with NMR studies suggesting that unphosphorylated RRs exist in equilibrium between inactive and active conformations (110) while interactions with the effector domain shift the equilibrium to the inactive state (27). The inward orientation of Y is predominant for most NarL subfamily members irrespective of phosphorylation status, thus is unlikely indicative of the active state, but rather a result of packing the α4-β5-α5 face with an accessory β6 strand, a structural feature found in many RRs of the NarL subfamily (20, 60, 83, 106). Therefore, the Y-T coupling mechanism is not universal in all RRs. Even for NtrC in which orientation switching has been observed, interconversion of the aromatic side chain has been suggested not to be involved in allosteric regulation because its rate of conversion is faster than the rate of active/inactive state conversion (109). RRs appear to be highly plastic for allosteric regulation with diverse mechanisms matching their sequence and structural features.

The Y and T residues are two of many residues that may participate in allosteric regulation. As discussed earlier, the phosphorylation site involves an intricate hydrogen-bond network with several residues from the β1-α1, β3-α3, β4-α4 and β5-α5 loops. It has been recognized that interactions, such as salt bridges and van der Waals contacts, of residues at D+1,

PeerJ Preprints | https://doi.org/10.7287/peerj.preprints.27554v2 | CC BY 4.0 Open Access | rec: 21 Mar 2019, publ: 21 Mar 2019

T+1, T+2, K and other positions can impact loop conformations and propagate the conformational changes to different areas of the REC domain (5, 14, 20, 44, 70, 106). Conformations with only subsets of active site residues at proper hydrogen-bonding positions have been discovered for many RRs (37, 95, 106) and are often referred to as meta-active states. A single RR can have multiple meta-active states with different combinations of loop conformations, as shown for NtrX (37). Unphosphorylated RRs can exist in equilibrium between the active state and multiple inactive or meta-active conformations and there are multiple pathways for transition to the active state (37, 44, 89). NMR relaxation data also support a model of segmental motions of multiple allosteric residues for activation of CheY, instead of a strict two-state switching model (70).

Just as phosphorylation shifts the equilibrium for effector domain regulation, the reverse scenario, with output domains affecting phosphorylation, has also been observed (8, 37). It has been suggested that adoption of an active conformation precedes phosphorylation (44, 53). Phosphorylation can be accelerated by any effect that increases the population of active conformation, such as relieving inhibition from the output domain by truncation, DNA binding in DBD-containing RRs, dimerization at high protein concentrations and HK-RR interaction (8, 9, 27, 28, 37, 66). Surface changes caused by these different interactions can propagate through the connecting βα loops to the phosphorylation site and other regions of the REC domain, increasing the active state population. One extraordinary example is DesR in which the HK-RR interaction can stabilize the active state of DesR and promote dimerization (66). Besides the phosphorylation-activated switch, interaction with the HK also functions as an allosteric switch to increase the population of active conformation for transcription activation. The same principle may be the basis for many phosphorylation-independent regulatory mechanisms.

PeerJ Preprints | https://doi.org/10.7287/peerj.preprints.27554v2 | CC BY 4.0 Open Access | rec: 21 Mar 2019, publ: 21 Mar 2019

Dimerization Modes and Corresponding Conformational Changes

Phosphorylation-promoted conformational changes are routinely identified by comparing X-ray or NMR structures obtained for unphosphorylated and BeF_3^--bound RRs. As shown in **Figure 5*a***, for the stand-alone RR CheY, significant differences in positions of backbone atoms occur at the β4-α4, β5-α5 loops and part of the α4-β5-α5 surface where CheY binds the FliM effector protein to regulate flagellar rotation. It is unsurprising that structural elements of the REC domain undergoing the largest rearrangements upon phosphorylation often correlate with protein-protein interaction surfaces, particularly, the dimer interface for DBD-containing RRs. Certain dimerization modes are popular for specific RR subfamilies with corresponding conformational changes.

A dimerization mode using the complete α4-β5-α5 surface is predominant in the OmpR subfamily (**Figure 5*b***). Dimer interaction involves salt bridges between pairs of highly conserved charged residues within the α4-β5-α5 region (104, 105). For the DrrB protein shown in **Figure 5*b***, conformational changes span the entire dimer surface. A Tyr residue is prevalent at the Y position (111) and switching of Tyr orientations has been observed. In several RRs (40, 78, 91), the hydroxyl group of Tyr is in close proximity to a polar residue from the DBD (**Figure 5*b right***), suggesting a potential role in effector inhibition. This is unlikely to be a common mechanism given the wide diversity of domain arrangements within the subfamily (8). RRs from the OmpR subfamily often recognize tandem DNA sites and two DBDs bind DNA in a head-to-tail manner (15, 48, 64, 76). The translational symmetry of DBDs coupled with the rotational symmetry of the REC domain predicts a flexible linker or different REC-DBD interfaces for individual RR monomers within the RR-DNA complex. Such asymmetry of REC-DBD interfaces has been observed for KdpE and PmrA (65, 76). However, NMR studies suggest that

PeerJ Preprints | https://doi.org/10.7287/peerj.preprints.27554v2 | CC BY 4.0 Open Access | rec: 21 Mar 2019, publ: 21 Mar 2019

the REC-DBD interaction observed for PmrA in the crystal structure is transient in solution (65). Additionally, alternative dimers involving α1-α5 (6, 71) or other surfaces (13) have also been discovered for unphosphorylated RRs but the physiological relevance of these dimers awaits further studies.

The NtrC subfamily of RRs displays two major modes of dimerization, with each involving different subsets of the α4-β5-α5 face (**Figure 5*c***). The α4-β5 dimer interface is often seen in phosphorylated RRs (**Table 1**) or unphosphorylated RRs with meta-active conformations (32, 37, 84). Another β5-α5 dimer is associated with inactive conformations (36, 84), as indicated by the outward orientation of the Phe residue at the Y position. Dimer interaction centers around the β5-α5 face, sometimes with a slightly tilted α5 helix in contact with both β5 and α4. Formation of the inactive β5-α5 dimer is believed to inhibit the AAA,+ ATPase output domain from oligomerization and transcription initiation (10, 84). For the LytTR subfamily, structural information is limited and a dimer also involving the α4-β5 subset of the α4-β5-α5 face has been observed for ComE (16).

Diverse dimerization modes have also been observed in the NarL subfamily. An α4-β5 dimer interface and the phosphorylation-dependent orientation of the Phe residue have been reported for the REC domain of FixJ (14). However, most RRs from the NarL subfamily show an α1-α5 dimer interface (**Table 1**) distinct from the widely used α4-β5-α5 surface (7, 20, 29, 60, 82, 106). The dimer interface mainly involves the α1 helix, the β1-α1 and β5-α5 loops (**Figure 5*d***). Correspondingly, significant structural rearrangements spanning to the α1 helix have been observed when apo- and BeF_3^--bound structures are compared. As discussed earlier, many RRs of the NarL subfamily display a constitutive inward orientation of the residue at the Y position, thus this residue is unlikely to be involved in allosteric regulation. Instead, different switching

PeerJ Preprints | https://doi.org/10.7287/peerj.preprints.27554v2 | CC BY 4.0 Open Access | rec: 21 Mar 2019, publ: 21 Mar 2019

mechanisms involving the T residue and other residues at α1, the β1-α1, β4-α4 and β5-α5 loops have been proposed for different RRs, such as VraR, DesR and RcsB (20, 60, 106). In addition to the α1-α5 dimer interface, the α4-β5-α5 surface is also remodeled to alter the positioning of the accessory β6 and α6 that are directly linked to the effector domain. Another dimer mode involving β6 and α6 is common (**Figure 5*d, right***) and several RRs, such as VraR (60), DesR (106), Spr1814 (82) and LiaR (29), show both α1-α5 and β6-α6 dimer modes within a single crystal. It has been suggested that the β6-α6 dimer may help RRs to form higher order oligomers on DNA to bind arrays of DNA-binding sites (106). DNA-bound structures of RcsB again indicate an asymmetric dimer with different rotation symmetry axes for the REC and DBDs (38). Different relative positions of the REC and DBDs are frequently observed for different full length RRs. Asymmetry is believed to result from either different REC-DBD interactions (20, 38) or a flexible linker that enables different disposition or even domain-swap of individual domains trapped in crystals (29, 60).

5. RESPONSE REGULATOR – HISTIDINE KINASE INTERACTIONS

HK Conformational States

HKs have a modular architecture with a large variety of sensory domains (extracellular, transmembrane or cytoplasmic) linked to a conserved catalytic domain by one or more signal transducing domains (12, 69) (**Figure 1*a***). The cytoplasmic enzymatic core of HKs consists of a dimerization histidine phosphotransfer (DHp) domain and a catalytic ATP-binding (CA) domain. The DHp domain contains the conserved phosphorylatable His residue and mediates dimerization of the HK to form a 4-helix bundle that is essential for its activity (**Figure 6**). The DHp dimer is flanked by the two α/β catalytic CA domains containing the kinase active sites that

PeerJ Preprints | https://doi.org/10.7287/peerj.preprints.27554v2 | CC BY 4.0 Open Access | rec: 21 Mar 2019, publ: 21 Mar 2019

catalyze phosphoryl transfer from ATP to the His residues. Autophosphorylation of the HK provides a high-energy phorphoryl group for subsequent phosphotransfer to the RR. Most HKs also mediate dephosphorylation of their cognate RRs in order to modulate the output response.

Large conformational changes in HKs occur during transitions between kinase, phosphoryltranfer and phosphatase states. In the HisKA_3 subfamily of HKs (e.g. DesK of *Bacillus subtilis*), the switch between states involves a large rotation of the DHp domains, a mechanism that is less pronounced in the HisKA subfamily. Specific regulatory mechanisms have been described for individual HKs, including the stabilization of the phosphatase state by ligand binding (e.g. c-di-GMP binding on CckA) and the inhibition of the phosphatase state by a pH-dependent conformational switch (33, 62). In contrast to the different conformations of HKs, structures of HK-REC domain complexes determined to date indicate that REC domains bound to either phosphotransfer or phosphatase states of HKs have similar conformations, with the REC domain displaying a meta-active conformation, as defined in the previous section.

Partner Recognition and Specificity

Specificity of HK-RR pairs is crucial for the integrity of signaling pathways, given the large number of different TCSs that typically exist in a single cell. Specificity within a pair is mediated by recognition residues that participate in HK-RR binding. These residues are located in helix α1 of the REC domain and in the two α helices of the HK DHp domain that contribute to the binding interface. Signaling pathways have been successfully rewired by substituting as few as three co-evolved specificity residues (88, 96). Additional strategies are employed to further ensure specificity of the pairs. For example, the phosphatase activity of HKs eliminates non-specific phosphorylation by non-cognate kinases or small molecule phosphodonors such as AcP.

PeerJ Preprints | https://doi.org/10.7287/peerj.preprints.27554v2 | CC BY 4.0 Open Access | rec: 21 Mar 2019, publ: 21 Mar 2019

The low-abundance of HKs relative to RRs also minimizes cross-phosphorylation between non-cognate pairs (57).

In an HK-RR complex, the REC domain inserts its α1 helix and β5-α5 loop between the two helices of the DHp domain, primarily contacting the DHp α1 helix that contains the phosphorylatable His residue. This conserved mode of binding buries the active site of the REC domain at the HK-RR interface (**Figure 6**). Thus, conserved residues of both the HK and RR form a substantial subset of the interface residues, with specificity being determined by a relatively small set of variable residues. In addition to these specificity residues in α1 of the REC domain and the two helices of the DHp domain, additional variable contacts can involve the β2-α2, β3-α3 and β4-α4 loops of the REC domain interacting with the CA domain, the *C*-terminal region of the DHp and the DHp-CA linker of the other protomer of the dimer (**Figure 6**) (21, 72, 74, 88, 107, 108, 114, 118, 122). Other contacts can occur between the REC domain and additional domains within the HK, increasing the specificity and/or stability of the pair (e.g. contacts between the PAS domain of ThkA and the RR TrrA) (118). These elements suggest that beyond the conserved REC-DHp interface that buries the active site, the binding interface can vary greatly in different HK-RR pairs.

A model based on structures of HK FixL and full-length RR FixJ suggests that the RR effector domain is free to move and does not participate in binding to the HK (116). However, a lack of structures of full-length RRs bound to HKs leaves open the question as to how effector domains might be positioned relative to REC domains and domains of the HK. Given the great diversity in REC-effector domain arrangements in different inactive RRs, it is possible that diversity exists in the ways effector domains interact in different HK-RR complexes. It is easy to envision how an effector domain could participate in the stability of the complex and/or the

PeerJ Preprints | https://doi.org/10.7287/peerj.preprints.27554v2 | CC BY 4.0 Open Access | rec: 21 Mar 2019, publ: 21 Mar 2019

efficiency of catalysis. Indeed, the meta-active conformation of the REC domain observed in HK-REC domain complexes might be a consequence of isolated REC domains being unhindered by REC-effector interactions that could bias conformational states.

Phosphotransfer State

Structural and biochemical studies of DesK-DesR complexes suggest that one HK dimer binds to one RR molecule in an asymmetric conformation. The DesK-DesR structure and a docking model of CpxA-CpxR in a putative phosphotransfer state show asymmetry within the HK dimer, with the CA domain of one monomer bound to the DHp domain of the other monomer, leaving the second CA domain untethered with enough space for RR binding to the DHp. Structural data from the DesK-DesR complex and from CpxA-CpxR model suggest that this highly dynamic state is coupled with autokinase activity, involves back-and-forth movements of the DHp and CA domains, and is modulated by REC domain binding (72, 107).

Phosphatase State

In contrast to the asymmetrical domain arrangements associated with phosphotransfer, HK-RR complexes in putative dephosphorylation states have symmetrical arrangements of the HK DHp and CA domains. The REC domains are also arranged symmetrically, each interacting with a DHp domain with a 2:2 HK:RR stoichiometry (62, 107). The HK in its phosphatase state is more rigid than in the phosphotransfer state, with the *N*-terminal coiled-coil of the DHp domains being highly stable.

Despite the large number of structures recently determined, the mechanistic details of the enzymatic reactions involving HKs and RRs are not fully understood. Discrimination between the phosphotransfer and phosphatase states that have been trapped in crystal structures still remains challenging. The situation is further complicated by distinct phosphatase mechanisms

PeerJ Preprints | https://doi.org/10.7287/peerj.preprints.27554v2 | CC BY 4.0 Open Access | rec: 21 Mar 2019, publ: 21 Mar 2019

454 used by HKs of different subtypes. A major limitation of current studies is the use of truncated
455 proteins, most notably the cytoplasmic domains of transmembrane HKs lacking sensor and
456 transmembrane regions that in intact proteins control the signaling states of HKs, and REC
457 domains of RRs in the absence of effector domains that are known to influence their
458 conformational equilibria. While conserved features of HK-RR interactions are beginning to be
459 elucidated, variations on the theme are anticipated. Similar to many other aspects of TCS
460 structure and function, it is likely that the great variety of domain architectures in TCS proteins
461 enable different modes of HK-RR interactions and regulatory mechanisms that are adapted to
462 individual HK-RR pairs.
463

464 **6. NON-CANONICAL MODES OF RR REGULATION**

465 The canonical mechanism for regulation of RR activity involves phosphorylation at a conserved
466 Asp in the REC domain, stabilizing an active conformation that enables effector domain function.
467 Regulation of RR activity, in addition to or in place of Asp phosphorylation, potentially can be
468 achieved in many different ways including post-translational modifications at other sites that bias
469 the conformational equilibrium of the REC domain or directly alter effector domain function,
470 interactions that lower the energetic barrier for transition to an active conformation, ligand
471 binding to the RR, and regulation of expression to control RR levels and thus dimerization or
472 oligomerization. Indeed, each of these strategies has been observed and a few examples are
473 described below.

474 Reversible protein acetylation is known to regulate metabolic enzymes and transcription
475 in bacteria (49) and was documented in CheY more than 20 years ago (90). Enzyme catalyzed
476 acetylation of CheY at K91 and K106 increases in response to acetate and promotes clockwise

PeerJ Preprints | https://doi.org/10.7287/peerj.preprints.27554v2 | CC BY 4.0 Open Access | rec: 21 Mar 2019, publ: 21 Mar 2019

flagellar rotation, with acetylation at K91 proposed to alter conformational dynamics of the β4α4 loop (39). Autoacetylation with AcCoA as acetyl donor at other sites in CheY is thought to link chemotaxis to the metabolic state of the cell (120). Another well-characterized example of acetylation occurs in *E. coli* transcription factor RcsB. Acetylation of K154, a residue in the helix-turn-helix motif that interacts with a phosphate in the DNA backbone, disrupts DNA binding, down-regulates expression of the acid stress response genes, and compromises survival in acidic conditions (22, 51). It should be noted that the stoichiometry of acetylation has not been determined, thus physiological effects observed with mutations that mimic fully unmodified or acetylated states might overestimate regulation that occurs in wild-type cells. A proteomics study in *E. coli* documented acetylation of seven RRs: ArcA, CheY, CpxR, EvgA, NarL, OmpR and RcsB (22). The *E. coli* genome encodes 26 putative Gcn5 *N*-acetyltransferases (GNATs) and a single known deacetylase (CobB) (49). While the best-characterized acetyltransferase, PatZ, is proposed to mediate a global strategy linking regulation to metabolic state, the large number of acetyltransferases raises the possibility of substrate specificity that might enable system-specific signaling mechanisms.

Signal-induced, HK-dependent, phosphorylation-independent monomer to dimer activation has been observed for several RR transcription factors. In the extensively studied *B. subtilis* system, binding of DesR to DesK promotes an active conformation of DesR. At sufficiently high RR concentrations and with a slow active to inactive state transition, dimerization can occur upon release of the RR from the HK with subsequent stabilization of the dimer upon DNA binding (106). Similar phosphorylation-independent activation of OmpR by HK EnvZ has been observed in acidic conditions (23). Cyanobacterial transcription factor NblR contains a conserved Asp, but lacks other residues necessary for phosphorylation. HK NblS is

PeerJ Preprints | https://doi.org/10.7287/peerj.preprints.27554v2 | CC BY 4.0 Open Access | rec: 21 Mar 2019, publ: 21 Mar 2019

500 required for phosphorylation-independent activation of NblR. However, no NblS-NblR
501 interactions have been detected and the activating monomer to dimer transition is postulated to
502 be promoted by another protein partner (93).

503 Multiple strategies have been identified for regulation of orphan RRs that lack a
504 conserved Asp and/or other conserved residues necessary for phosphorylation. In streptomycetes,
505 two atypical RR transcription factors that lack residues necessary for phosphorylation, JadR1 and
506 RedZ, are regulated by the end products of the antibiotic biosynthetic pathways they control. The
507 antibiotic JdB binds directly to the JadR1 REC domain, disrupting DNA binding (112). A
508 different strategy is used by *Helicobacter pylori* HP1043, which exists as a constitutively active
509 dimer *in vitro* with a crystal structure similar to that of other activated OmpR subfamily
510 members (50). Levels of HP1043 are regulated both transcriptionally and post-transcriptionally
511 leading to speculation that control of expression of this constitutively active RR may be the sole
512 mechanism for regulating HP1403 activity (75).

513 Combinations of these mechanisms create even more strategies. *Streptomyces coelicolor*
514 GlnR, which regulates genes for nitrogen assimilation, is an orphan OmpR subfamily RR that
515 lacks residues for Asp phosphorylation and forms a constitutive α4-β5-α5 dimer (61). GlnR is
516 phosphorylated at 6 Ser/Thr sites in the DNA-binding domain under N-rich conditions,
517 disrupting DNA binding. GlnR is also acetylated at multiple Lys residues in the DNA-binding
518 domain, with acetylation enhancing DNA binding (4).

519

520 **7. CONCLUDING REMARKS**

521 When the structure of an RR REC domain was first reported thirty years ago, a central question
522 was how this single conserved domain could regulate responses as diverse as flagellar rotation,

PeerJ Preprints | https://doi.org/10.7287/peerj.preprints.27554v2 | CC BY 4.0 Open Access | rec: 21 Mar 2019, publ: 21 Mar 2019

transcription, and enzyme activity. The answer that emerged defined a mechanism that was both simple and versatile. The small α/β REC domain exists in equilibrium between two primary conformations with phosphorylation stabilizing an active conformation. This phosphorylation-regulated switch enables regulatory strategies via any type of activating or inhibitory macromolecular interactions that discriminate between the two states. Hundreds of structures of RRs have provided descriptions of the conformations of REC domains in inactive and active states, interactions with effector domains, DNA, HKs and auxiliary proteins. These structures provide a foundation for identifying conserved features as well as specific variations in individual RRs. Beyond the universally conserved enzymatic mechanisms facilitated by configurations at the active site, other features such as Y-T coupling, regions of conformational perturbations, domain arrangements and modes of DNA binding show distinct trends among RRs within specific subfamilies.

Numerous variations on most every feature of RRs have been observed and undoubtedly, many more remain to be discovered. The plasticity of the REC domain and versatility of RR design allow an almost unlimited array of adaptations to fit the needs of individual signaling systems. Defining details of how specific structural features impact function is important for interpreting the nuances of RR behavior within specific TCSs as well as for pursuit of applied projects such as development of antimicrobial therapeutics or the engineering of synthetic biosensing pathways.

Our current understanding of RR structure is largely informed by compiling information derived from many partial structural descriptions of different RRs. Very few structures are available for full-length multi-domain RRs in both inactive and active states. The crystal structures that do exist are constrained by the limitations of the methodology, specifically the

PeerJ Preprints | https://doi.org/10.7287/peerj.preprints.27554v2 | CC BY 4.0 Open Access | rec: 21 Mar 2019, publ: 21 Mar 2019

capture of single discrete states that do not reflect conformational distributions and the potential promotion of inter- and/or intra-molecular interactions that are influenced by the high concentrations of proteins used in crystallization and/or stabilization of conformations necessary for crystallization and lattice interactions. While NMR studies have provided information about dynamics and conformational distributions in solution, size limitations have mostly precluded studies of full-length RRs, dimers, oligomers and complexes of RRs with HKs or other macromolecular partners. Thus, while structures unambiguously define allowable states, it is important to keep in mind the conformationally dynamic nature of RRs and the potential influence of associated domains and macromolecular partners when interpreting structures determined by methodologies with technical limitations. The emergence of new structural methods such as high-resolution cryo-electron microscopy promise to provide solutions to some of these challenges.

DISCLOSURE STATEMENT

The authors are not aware of any affiliations, memberships, funding, or financial holdings that might be perceived as affecting the objectivity of this review.

ACKNOWLEDGMENTS

Research in the Stock laboratory is supported by grant R01 GM47958 from the National Institutes of Health. S.B. was supported in part by the Foundation pour la Recherche Médicale (FRM) Grant SPE201803005070.

PeerJ Preprints | https://doi.org/10.7287/peerj.preprints.27554v2 | CC BY 4.0 Open Access | rec: 21 Mar 2019, publ: 21 Mar 2019

LITERATURE CITED

1. Alexander RP, Lowenthal AC, Harshey RM, Ottemann KM. 2010. CheV: CheW-like coupling proteins at the core of the chemotaxis signaling network. *Trends Microbiol.* 18:494-503
2. Alvarez AF, Barba-Ostria C, Silva-Jimenez H, Georgellis D. 2016. Organization and mode of action of two component system signaling circuits from the various kingdoms of life. *Environ. Microbiol.* 18:3210-26
3. Amin M, Kothamachu VB, Feliu E, Scharf BE, Porter SL, Soyer OS. 2014. Phosphate sink containing two-component signaling systems as tunable threshold devices. *PLoS Comput. Biol.* 10:e1003890
4. Amin R, Franz-Wachtel M, Tiffert Y, Heberer M, Meky M, et al. 2016. Post-translational serine/threonine phosphorylation and lysine acetylation: a novel regulatory aspect of the global nitrogen response regulator GlnR in *S. coelicolor* M145. *Front. Mol. Biosci.* 3:38
5. Amor BR, Schaub MT, Yaliraki SN, Barahona M. 2016. Prediction of allosteric sites and mediating interactions through bond-to-bond propensities. *Nat. Commun.* 7:12477
6. Bachhawat P, Swapna GV, Montelione GT, Stock AM. 2005. Mechanism of activation for transcription factor PhoB suggested by different modes of dimerization in the inactive and active states. *Structure* 13:1353-63
7. Baikalov I, Schröder I, Kaczor-Grzeskowiak M, Grzeskowiak K, Gunsalus RP, Dickerson RE. 1996. Structure of the *Escherichia coli* response regulator NarL. *Biochemistry* 35:11053-61

PeerJ Preprints | https://doi.org/10.7287/peerj.preprints.27554v2 | CC BY 4.0 Open Access | rec: 21 Mar 2019, publ: 21 Mar 2019

8. Barbieri CM, Mack TR, Robinson VL, Miller MT, Stock AM. 2010. Regulation of response regulator autophosphorylation through interdomain contacts. *J. Biol. Chem.* 285:32325-35

9. Barbieri CM, Wu T, Stock AM. 2013. Comprehensive analysis of OmpR phosphorylation, dimerization, and DNA binding supports a canonical model for activation. *J. Mol. Biol.* 425:1612-26

10. Batchelor JD, Doucleff M, Lee CJ, Matsubara K, De Carlo S, et al. 2008. Structure and regulatory mechanism of *Aquifex aeolicus* NtrC4: variability and evolution in bacterial transcriptional regulation. *J. Mol. Biol.* 384:1058-75

11. Battesti A, Majdalani N, Gottesman S. 2011. The RpoS-mediated general stress response in *Escherichia coli*. *Annu. Rev. Microbiol.* 65:189-213

12. Bhate MP, Molnar KS, Goulian M, DeGrado WF. 2015. Signal transduction in histidine kinases: insights from new structures. *Structure* 23:981-94

13. Birck C, Chen Y, Hulett FM, Samama JP. 2003. The crystal structure of the phosphorylation domain in PhoP reveals a functional tandem association mediated by an asymmetric interface. *J. Bacteriol.* 185:254-61

14. Birck C, Mourey L, Gouet P, Fabry B, Schumacher J, et al. 1999. Conformational changes induced by phosphorylation of the FixJ receiver domain. *Structure* 7:1505-15

15. Blanco AG, Sola M, Gomis-Ruth FX, Coll M. 2002. Tandem DNA recognition by PhoB, a two-component signal transduction transcriptional activator. *Structure* 10:701-13

16. Boudes M, Sanchez D, Graille M, van Tilbeurgh H, Durand D, Quevillon-Cheruel S. 2014. Structural insights into the dimerization of the response regulator ComE from *Streptococcus pneumoniae*. *Nucleic Acids Res.* 42:5302-13

PeerJ Preprints | https://doi.org/10.7287/peerj.preprints.27554v2 | CC BY 4.0 Open Access | rec: 21 Mar 2019, publ: 21 Mar 2019

613 17. Bourret RB. 2010. Receiver domain structure and function in response regulator proteins.
614 *Curr. Opin. Microbiol.* 13:142-49
615 18. Burley SK, Berman HM, Kleywegt GJ, Markley JL, Nakamura H, Velankar S. 2017.
616 Protein Data Bank (PDB): The single global macromolecular structure archive. *Methods*
617 *Mol. Biol.* 1607:627-41
618 19. Capra EJ, Perchuk BS, Skerker JM, Laub MT. 2012. Adaptive mutations that prevent
619 crosstalk enable the expansion of paralogous signaling protein families. *Cell* 150:222-32
620 20. Casino P, Miguel-Romero L, Huesa J, Garcia P, Garcia-Del Portillo F, Marina A. 2018.
621 Conformational dynamism for DNA interaction in the *Salmonella* RcsB response regulator.
622 *Nucleic Acids Res.* 46:456-72
623 21. Casino P, Rubio V, Marina A. 2009. Structural insight into partner specificity and
624 phosphoryl transfer in two-component signal transduction. *Cell* 139:325-36
625 22. Castano-Cerezo S, Bernal V, Post H, Fuhrer T, Cappadona S, et al. 2014. Protein
626 acetylation affects acetate metabolism, motility and acid stress response in *Escherichia coli*.
627 *Mol. Syst. Biol.* 10:762
628 23. Chakraborty S, Winardhi RS, Morgan LK, Yan J, Kenney LJ. 2017. Non-canonical
629 activation of OmpR drives acid and osmotic stress responses in single bacterial cells. *Nat.*
630 *Commun.* 8:1587
631 24. Childers WS, Xu Q, Mann TH, Mathews, II, Blair JA, et al. 2014. Cell fate regulation
632 governed by a repurposed bacterial histidine kinase. *PLoS Biol.* 12:e1001979
633 25. Cho HS, Lee SY, Yan D, Pan X, Parkinson JS, et al. 2000. NMR structure of activated
634 CheY. *J. Mol. Biol.* 297:543-51

PeerJ Preprints | https://doi.org/10.7287/peerj.preprints.27554v2 | CC BY 4.0 Open Access | rec: 21 Mar 2019, publ: 21 Mar 2019

635 26. Choudhury HG, Beis K. 2013. The dimeric form of the unphosphorylated response
636 regulator BaeR. *Protein Sci.* 22:1287-93
637 27. Correa F, Gardner KH. 2016. Basis of mutual domain inhibition in a bacterial response
638 regulator. *Cell Chem. Biol.* 23:945-54
639 28. Creager-Allen RL, Silversmith RE, Bourret RB. 2013. A link between dimerization and
640 autophosphorylation of the response regulator PhoB. *J. Biol. Chem.* 288:21755-69
641 29. Davlieva M, Tovar-Yanez A, DeBruler K, Leonard PG, Zianni MR, et al. 2016. An
642 adaptive mutation in *Enterococcus faecium* LiaR associated with antimicrobial peptide
643 resistance mimics phosphorylation and stabilizes LiaR in an activated state. *J. Mol. Biol.*
644 428:4503-19
645 30. de Been M, Tempelaars MH, van Schaik W, Moezelaar R, Siezen RJ, Abee T. 2010. A
646 novel hybrid kinase is essential for regulating the sigma(B)-mediated stress response of
647 *Bacillus cereus*. *Environ. Microbiol.* 12:730-45
648 31. Djordjevic S, Goudreau PN, Xu Q, Stock AM, West AH. 1998. Structural basis for
649 methylesterase CheB regulation by a phosphorylation-activated domain. *Proc. Natl. Acad.*
650 *Sci. USA* 95:1381-86
651 32. Doucleff M, Chen B, Maris AE, Wemmer DE, Kondrashkina E, Nixon BT. 2005. Negative
652 regulation of AAA+ ATPase assembly by two component receiver domains: a transcription
653 activation mechanism that is conserved in mesophilic and extremely hyperthermophilic
654 bacteria. *J. Mol. Biol.* 353:242-55
655 33. Dubey BN, Lori C, Ozaki S, Fucile G, Plaza-Menacho I, et al. 2016. Cyclic di-GMP
656 mediates a histidine kinase/phosphatase switch by noncovalent domain cross-linking. *Sci.*
657 *Adv.* 2:e1600823

PeerJ Preprints | https://doi.org/10.7287/peerj.preprints.27554v2 | CC BY 4.0 Open Access | rec: 21 Mar 2019, publ: 21 Mar 2019

34. Dutta R, Inouye M. 1996. Reverse phosphotransfer from OmpR to EnvZ in a kinase$^-$/phosphatase$^+$ mutant of EnvZ (EnvZ$^-$N347D), a bifunctional signal transducer of *Escherichia coli*. *J. Biol. Chem.* 271:1424-29

35. El-Gebali S, Mistry J, Bateman A, Eddy SR, Luciani A, et al. 2018. The Pfam protein families database in 2019. *Nucleic Acids Res.*:[Epub ahead of print]

36. Fernandez I, Cornaciu I, Carrica MD, Uchikawa E, Hoffmann G, et al. 2017. Three-dimensional structure of full-length NtrX, an unusual member of the NtrC family of response regulators. *J. Mol. Biol.* 429:1192-212

37. Fernandez I, Otero LH, Klinke S, Carrica MDC, Goldbaum FA. 2015. Snapshots of conformational changes shed light into the NtrX receiver domain signal transduction mechanism. *J. Mol. Biol.* 427:3258-72

38. Filippova EV, Zemaitaitis B, Aung T, Wolfe AJ, Anderson WF. 2018. Structural basis for DNA recognition by the two-component response regulator RcsB. *MBio* 9:01993-17

39. Fraiberg M, Afanzar O, Cassidy CK, Gabashvili A, Schulten K, et al. 2015. CheY's acetylation sites responsible for generating clockwise flagellar rotation in *Escherichia coli*. *Mol. Microbiol.* 95:231-44

40. Friedland N, Mack TR, Yu M, Hung L-W, Terwilliger TC, et al. 2007. Domain orientation in the inactive response regulator *Mycobacterium tuberculosis* MtrA provides a barrier to activation. *Biochemistry* 46:6733-43

41. Galperin MY, Makarova KS, Wolf YI, Koonin EV. 2018. Phyletic distribution and lineage-specific domain architectures of archaeal two-component signal transduction systems. *J. Bacteriol.* 200:e00681-17

PeerJ Preprints | https://doi.org/10.7287/peerj.preprints.27554v2 | CC BY 4.0 Open Access | rec: 21 Mar 2019, publ: 21 Mar 2019

680 42. Gao R, Stock AM. 2010. Molecular strategies for phosphorylation-mediated regulation of
681 response regulator activity. *Curr. Opin. Microbiol.* 13:160-67
682 43. Gao R, Stock AM. 2017. Quantitative kinetic analyses of shutting off a two-component
683 system. *MBio* 8:e00412-17
684 44. Gardino AK, Villali J, Kivenson A, Lei M, Liu CF, et al. 2009. Transient non-native
685 hydrogen bonds promote activation of a signaling protein. *Cell* 139:1109-18
686 45. Gottschlich L, Bortfeld-Miller M, Gabelein C, Dintner S, Vorholt JA. 2018. Phosphorelay
687 through the bifunctional phosphotransferase PhyT controls the general stress response in an
688 alphaproteobacterium. *PLoS Genet.* 14:e1007294
689 46. Grimshaw CE, Huang S, Hanstein CG, Strauch MA, Burbulys D, et al. 1998. Synergistic
690 kinetic interactions between components of the phosphorelay controlling sporulation in
691 *Bacillus subtilis*. *Biochemistry* 37:1365-75
692 47. Hastings CA, Lee SY, Cho HS, Yan D, Kustu S, Wemmer DE. 2003. High-resolution
693 solution structure of the beryllofluoride-activated NtrC receiver domain. *Biochemistry*
694 42:9081-90
695 48. He X, Wang L, Wang S. 2016. Structural basis of DNA sequence recognition by the
696 response regulator PhoP in *Mycobacterium tuberculosis*. *Sci Rep* 6:24442
697 49. Hentchel KL, Escalante-Semerena JC. 2015. Acylation of biomolecules in prokaryotes: a
698 widespread strategy for the control of biological function and metabolic stress. *Microbiol.*
699 *Mol. Biol. Rev.* 79:321-46
700 50. Hong E, Lee HM, Ko H, Kim DU, Jeon BY, et al. 2007. Structure of an atypical orphan
701 response regulator protein supports a new phosphorylation-independent regulatory
702 mechanism. *J. Biol. Chem.* 282:20667-75

PeerJ Preprints | https://doi.org/10.7287/peerj.preprints.27554v2 | CC BY 4.0 Open Access | rec: 21 Mar 2019, publ: 21 Mar 2019

703 51. Hu LI, Chi BK, Kuhn ML, Filippova EV, Walker-Peddakotla AJ, et al. 2013. Acetylation
704 of the response regulator RcsB controls transcription from a small RNA promoter. *J.*
705 *Bacteriol.* 195:4174-86
706 52. Huynh TN, Stewart V. 2011. Negative control in two-component signal transduction by
707 transmitter phosphatase activity. *Mol. Microbiol.* 82:275-86
708 53. Immormino RM, Silversmith RE, Bourret RB. 2016. A variable active site residue
709 influences the kinetics of response regulator phosphorylation and dephosphorylation.
710 *Biochemistry* 55:5595-609
711 54. Inclan YF, Laurent S, Zusman DR. 2008. The receiver domain of FrzE, a CheA-CheY
712 fusion protein, regulates the CheA histidine kinase activity and downstream signalling to
713 the A- and S-motility systems of *Myxococcus xanthus*. *Mol. Microbiol.* 68:1328-39
714 55. King-Scott J, Nowak E, Mylonas E, Panjikar S, Roessle M, et al. 2007. The structure of a
715 full-length response regulator from *Mycobacterium tuberculosis* in a stabilized three-
716 dimensional domain-swapped, activated state. *J. Biol. Chem.* 282:37717-29
717 56. Lau J, Hernandez-Alicea L, Vass RH, Chien P. 2015. A phosphosignaling adaptor primes
718 the AAA+ protease ClpXP to drive cell cycle-regulated proteolysis. *Mol. Cell* 59:104-16
719 57. Laub MT, Goulian M. 2007. Specificity in two-component signal transduction pathways.
720 *Annu. Rev. Genet.* 41:121-45
721 58. Lee SY, De La Torre A, Yan D, Kustu S, Nixon BT, Wemmer DE. 2003. Regulation of the
722 transcriptional activator NtrC1: structural studies of the regulatory and AAA^+ ATPase
723 domains. *Genes Dev.* 17:2552-63
724 59. Lehman MK, Bose JL, Sharma-Kuinkel BK, Moormeier DE, Endres JL, et al. 2015.
725 Identification of the amino acids essential for LytSR-mediated signal transduction in

PeerJ Preprints | https://doi.org/10.7287/peerj.preprints.27554v2 | CC BY 4.0 Open Access | rec: 21 Mar 2019, publ: 21 Mar 2019

Staphylococcus aureus and their roles in biofilm-specific gene expression. *Mol. Microbiol.* 95:723-37

60. Leonard PG, Golemi-Kotra D, Stock AM. 2013. Phosphorylation-dependent conformational changes and domain rearrangements in *Staphylococcus aureus* VraR activation. *Proc. Natl. Acad. Sci. USA* 110:8525-30

61. Lin W, Wang Y, Han X, Zhang Z, Wang C, et al. 2014. Atypical OmpR/PhoB subfamily response regulator GlnR of actinomycetes functions as a homodimer, stabilized by the unphosphorylated conserved Asp-focused charge interactions. *J. Biol. Chem.* 289:15413-25

62. Liu Y, Rose J, Huang S, Hu Y, Wu Q, et al. 2017. A pH-gated conformational switch regulates the phosphatase activity of bifunctional HisKA-family histidine kinases. *Nat. Commun.* 8:2104

63. Lori C, Kaczmarczyk A, de Jong I, Jenal U. 2018. A single-domain response regulator functions as an integrating hub to coordinate general stress response and development in alphaproteobacteria. *MBio* 9:e00809-18

64. Lou YC, Wang I, Rajasekaran M, Kao YF, Ho MR, et al. 2014. Solution structure and tandem DNA recognition of the C-terminal effector domain of PmrA from *Klebsiella pneumoniae*. *Nucleic Acids Res.* 42:4080-93

65. Lou YC, Weng TH, Li YC, Kao YF, Lin WF, et al. 2015. Structure and dynamics of polymyxin-resistance-associated response regulator PmrA in complex with promoter DNA. *Nat. Commun.* 6:8838

66. Luebke JL, Eaton DS, Sachleben JR, Crosson S. 2018. Allosteric control of a bacterial stress response system by an anti-sigma factor. *Mol. Microbiol.* 107:164-79

PeerJ Preprints | https://doi.org/10.7287/peerj.preprints.27554v2 | CC BY 4.0 Open Access | rec: 21 Mar 2019, publ: 21 Mar 2019

748 67. Lukat GS, McCleary WR, Stock AM, Stock JB. 1992. Phosphorylation of bacterial
749 response regulator proteins by low molecular weight phospho-donors. *Proc. Natl. Acad. Sci.*
750 *USA* 89:718-22
751 68. Martinez-Hackert E, Stock AM. 1997. Structural relationships in the OmpR family of
752 winged-helix transcription factors. *J. Mol. Biol.* 269:301-12
753 69. Mascher T, Helmann JD, Unden G. 2006. Stimulus perception in bacterial signal-
754 transducing histidine kinases. *Microbiol. Mol. Biol. Rev.* 70:910-38
755 70. McDonald LR, Boyer JA, Lee AL. 2012. Segmental motions, not a two-state concerted
756 switch, underlie allostery in CheY. *Structure* 20:1363-73
757 71. Mechaly AE, Haouz A, Sassoon N, Buschiazzo A, Betton JM, Alzari PM. 2018.
758 Conformational plasticity of the response regulator CpxR, a key player in
759 Gammaproteobacteria virulence and drug-resistance. *J. Struct. Biol.* 204:165-71
760 72. Mechaly AE, Soto Diaz S, Sassoon N, Buschiazzo A, Betton JM, Alzari PM. 2017.
761 Structural coupling between autokinase and phosphotransferase reactions in a bacterial
762 histidine kinase. *Structure* 25:939-44.e3
763 73. Milani M, Leoni L, Rampioni G, Zennaro E, Ascenzi P, Bolognesi M. 2005. An active-like
764 structure in the unphosphorylated StyR response regulator suggests a phosphorylation-
765 dependent allosteric activation mechanism. *Structure* 13:1289-97
766 74. Mo G, Zhou H, Kawamura T, Dahlquist FW. 2012. Solution structure of a complex of the
767 histidine autokinase CheA with its substrate CheY. *Biochemistry* 51:3786-98
768 75. Müller S, Pflock M, Schär J, Kennard S, Beier D. 2007. Regulation of expression of
769 atypical orphan response regulators of *Helicobacter pylori*. *Microbiol. Res.* 162:1-14

PeerJ Preprints | https://doi.org/10.7287/peerj.preprints.27554v2 | CC BY 4.0 Open Access | rec: 21 Mar 2019, publ: 21 Mar 2019

770 76. Narayanan A, Paul LN, Tomar S, Patil DN, Kumar P, Yernool DA. 2012. Structure-
771 function studies of DNA binding domain of response regulator KdpE reveals equal affinity
772 interactions at DNA half-sites. *PLoS One* 7:e30102
773 77. Nesper J, Hug I, Kato S, Hee CS, Habazettl JM, et al. 2017. Cyclic di-GMP differentially
774 tunes a bacterial flagellar motor through a novel class of CheY-like regulators. *Elife* 6
775 78. Nowak E, Panjikar S, Konarev P, Svergun DI, Tucker PA. 2006. The structural basis of
776 signal transduction for the response regulator PrrA from *Mycobacterium tuberculosis*. *J.*
777 *Biol. Chem.* 281:9659-66
778 79. O'Hara BP, Norman RA, Wan PT, Roe SM, Barrett TE, et al. 1999. Crystal structure and
779 induction mechanism of AmiC-AmiR: a ligand-regulated transcription antitermination
780 complex. *EMBO J.* 18:5175-86
781 80. Page SC, Immormino RM, Miller TH, Bourret RB. 2016. Experimental analysis of
782 functional variation within protein families: receiver domain autodephosphorylation
783 kinetics. *J. Bacteriol.* 198:2483-93
784 81. Parashar V, Mirouze N, Dubnau DA, Neiditch MB. 2011. Structural basis of response
785 regulator dephosphorylation by Rap phosphatases. *PLoS Biol.* 9:e1000589
786 82. Park AK, Lee JH, Chi YM, Park H. 2016. Structural characterization of the full-length
787 response regulator spr1814 in complex with a phosphate analogue reveals a novel
788 conformational plasticity of the linker region. *Biochem. Biophys. Res. Commun.* 473:625-9
789 83. Park AK, Moon JH, Lee KS, Chi YM. 2012. Crystal structure of receiver domain of
790 putative NarL family response regulator spr1814 from *Streptococcus pneumoniae* in the
791 absence and presence of the phosphoryl analog beryllofluoride. *Biochem. Biophys. Res.*
792 *Commun.* 421:403-7

PeerJ Preprints | https://doi.org/10.7287/peerj.preprints.27554v2 | CC BY 4.0 Open Access | rec: 21 Mar 2019, publ: 21 Mar 2019

793 84. Park S, Meyer M, Jones AD, Yennawar HP, Yennawar NH, Nixon BT. 2002. Two-
794 component signaling in the AAA^+ ATPase DctD: binding Mg^{2+} and BeF_3^- selects between
795 alternate dimeric states of the receiver domain. *FASEB J.* 16:1964-66
796 85. Patel K, Golemi-Kotra D. 2015. Signaling mechanism by the *Staphylococcus aureus* two-
797 component system LytSR: role of acetyl phosphate in bypassing the cell membrane
798 electrical potential sensor LytS. *F1000Res.* 4:79
799 86. Pazy Y, Motaleb MA, Guarnieri MT, Charon NW, Zhao R, Silversmith RE. 2010. Identical
800 phosphatase mechanisms achieved through distinct modes of binding phosphoprotein
801 substrate. *Proc. Natl. Acad. Sci. USA* 107:1924-29
802 87. Pazy Y, Wollish AC, Thomas SA, Miller PJ, Collins EJ, et al. 2009. Matching biochemical
803 reaction kinetics to the timescales of life: structural determinants that influence the
804 autodephosphorylation rate of response regulator proteins. *J. Mol. Biol.* 392:1205-20
805 88. Podgornaia AI, Laub MT. 2013. Determinants of specificity in two-component signal
806 transduction. *Curr. Opin. Microbiol.* 16:156-62
807 89. Pontiggia F, Pachov DV, Clarkson MW, Villali J, Hagan MF, et al. 2015. Free energy
808 landscape of activation in a signalling protein at atomic resolution. *Nat. Commun.* 6:7284
809 90. Ramakrishnan R, Schuster M, Bourret RB. 1998. Acetylation at Lys-92 enhances signaling
810 by the chemotaxis response regulator protein CheY. *Proc. Natl. Acad. Sci. USA* 95:4918-23
811 91. Robinson VL, Wu T, Stock AM. 2003. Structural analysis of the domain interface in DrrB,
812 a response regulator of the OmpR/PhoB subfamily. *J. Bacteriol.* 185:4186-94
813 92. Romling U, Gomelsky M, Galperin MY. 2005. C-di-GMP: the dawning of a novel bacterial
814 signalling system. *Mol. Microbiol.* 57:629-39

PeerJ Preprints | https://doi.org/10.7287/peerj.preprints.27554v2 | CC BY 4.0 Open Access | rec: 21 Mar 2019, publ: 21 Mar 2019

93. Ruiz D, Salinas P, Lopez-Redondo ML, Cayuela ML, Marina A, Contreras A. 2008. Phosphorylation-independent activation of the atypical response regulator NblR. *Microbiology* 154:3002-15

94. Sidote DJ, Barbieri CM, Wu T, Stock AM. 2008. Structure of the *Staphylococcus aureus* AgrA LytTR domain bound to DNA reveals a beta fold with an unusual mode of binding. *Structure* 16:727-35

95. Simonovic M, Volz K. 2001. A distinct meta-active conformation in the 1.1-Å resolution structure of wild-type apoCheY. *J. Biol. Chem.* 276:28637-40

96. Skerker JM, Perchuk BS, Siryaporn A, Lubin EA, Ashenberg O, et al. 2008. Rewiring the specificity of two-component signal transduction systems. *Cell* 133:1043-54

97. Sourjik V, Schmitt R. 1996. Different roles of CheY1 and CheY2 in the chemotaxis of *Rhizobium meliloti*. *Mol. Microbiol.* 22:427-36

98. Sourjik V, Schmitt R. 1998. Phosphotransfer between CheA, CheY1, and CheY2 in the chemotaxis signal transduction chain of *Rhizobium meliloti*. *Biochemistry* 37:2327-35

99. Stock AM, Robinson VL, Goudreau PN. 2000. Two-component signal transduction. *Annu. Rev. Biochem.* 69:183-215

100. Surette MG, Levit M, Liu Y, Lukat G, Ninfa EG, et al. 1996. Dimerization is required for the activity of the protein histidine kinase CheA that mediates signal transduction in bacterial chemotaxis. *J. Biol. Chem.* 271:939-45

101. Thomas SA, Brewster JA, Bourret RB. 2008. Two variable active site residues modulate response regulator phosphoryl group stability. *Mol. Microbiol.* 69:453-65

PeerJ Preprints | https://doi.org/10.7287/peerj.preprints.27554v2 | CC BY 4.0 Open Access | rec: 21 Mar 2019, publ: 21 Mar 2019

836 102. Thomas SA, Immormino RM, Bourret RB, Silversmith RE. 2013. Nonconserved active site
837 residues modulate CheY autophosphorylation kinetics and phosphodonor preference.
838 *Biochemistry* 52:2262-73
839 103. Tindall MJ, Porter SL, Maini PK, Armitage JP. 2010. Modeling chemotaxis reveals the role
840 of reversed phosphotransfer and a bi-functional kinase-phosphatase. *PLoS Comput. Biol.* 6
841 104. Toro-Roman A, Mack TR, Stock AM. 2005. Structural analysis and solution studies of the
842 activated regulatory domain of the response regulator ArcA: a symmetric dimer mediated
843 by the α4-β5-α5 face. *J. Mol. Biol.* 349:11-26
844 105. Toro-Roman A, Wu T, Stock AM. 2005. A common dimerization interface in bacterial
845 response regulators KdpE and TorR. *Protein Sci.* 14:3077-388
846 106. Trajtenberg F, Albanesi D, Ruetalo N, Botti H, Mechaly AE, et al. 2014. Allosteric
847 activation of bacterial response regulators: the role of the cognate histidine kinase beyond
848 phosphorylation. *MBio* 5:e02105
849 107. Trajtenberg F, Imelio JA, Machado MR, Larrieux N, Marti MA, et al. 2016. Regulation of
850 signaling directionality revealed by 3D snapshots of a kinase:regulator complex in action.
851 *Elife* 5:e21422
852 108. Varughese KI. 2005. Conformational changes of Spo0F along the phosphotransfer pathway.
853 *J. Bacteriol.* 187:8221-27
854 109. Villali J, Pontiggia F, Clarkson MW, Hagan MF, Kern D. 2014. Evidence against the "Y-T
855 coupling" mechanism of activation in the response regulator NtrC. *J. Mol. Biol.* 426:1554-
856 67
857 110. Volkman BF, Lipson D, Wemmer DE, Kern D. 2001. Two-state allosteric behavior in a
858 single domain signaling protein. *Science* 291:2429-33

PeerJ Preprints | https://doi.org/10.7287/peerj.preprints.27554v2 | CC BY 4.0 Open Access | rec: 21 Mar 2019, publ: 21 Mar 2019

111. Volz K. 1993. Structural conservation in the CheY superfamily. *Biochemistry* 32:11741-53

112. Wang L, Tian X, Wang J, Yang H, Fan K, et al. 2009. Autoregulation of antibiotic biosynthesis by binding of the end product to an atypical response regulator. *Proc. Natl. Acad. Sci. USA* 106:8617-22

113. Wheeler TJ, Clements J, Finn RD. 2014. Skylign: a tool for creating informative, interactive logos representing sequence alignments and profile hidden Markov models. *BMC Bioinformatics* 15:7

114. Willett JW, Herrou J, Briegel A, Rotskoff G, Crosson S. 2015. Structural asymmetry in a conserved signaling system that regulates division, replication, and virulence of an intracellular pathogen. *Proc .Natl. Acad. Sci. USA* 112:E3709-18

115. Wolfe AJ. 2010. Physiologically relevant small phosphodonors link metabolism to signal transduction. *Curr. Opin. Microbiol.* 13:204-9

116. Wright GSA, Saeki A, Hikima T, Nishizono Y, Hisano T, et al. 2018. Architecture of the complete oxygen-sensing FixL-FixJ two-component signal transduction system. *Sci. Signal.* 11

117. Wu J, Ohta N, Newton A. 1998. An essential, multicomponent signal transduction pathway required for cell cycle regulation in *Caulobacter*. *Proc. Natl. Acad. Sci. USA* 95:1443-48

118. Yamada S, Sugimoto H, Kobayashi M, Ohno A, Nakamura H, Shiro Y. 2009. Structure of PAS-linked histidine kinase and the response regulator complex. *Structure* 17:1333-44

119. Yan D, Cho HS, Hastings CA, Igo MM, Lee SY, et al. 1999. Beryllofluoride mimics phosphorylation of NtrC and other bacterial response regulators. *Proc. Natl. Acad. Sci. USA* 96:14789-94

PeerJ Preprints | https://doi.org/10.7287/peerj.preprints.27554v2 | CC BY 4.0 Open Access | rec: 21 Mar 2019, publ: 21 Mar 2019

120. Yan J, Barak R, Liarzi O, Shainskaya A, Eisenbach M. 2008. *In vivo* acetylation of CheY, a response regulator in chemotaxis of *Escherichia coli*. *J. Mol. Biol.* 376:1260-71

121. Zapf J, Madhusudan M, Grimshaw CE, Hoch JA, Varughese KI, Whiteley JM. 1998. A source of response regulator autophosphatase activity: the critical role of a residue adjacent to the Spo0F autophosphorylation active site. *Biochemistry* 37:7725-32

122. Zapf J, Sen U, Madhusudan, Hoch JA, Varughese KI. 2000. A transient interaction between two phosphorelay proteins trapped in a crystal lattice reveals the mechanism of molecular recognition and phosphotransfer in signal transduction. *Structure* 8:851-62

123. Zhao R, Collins EJ, Bourret RB, Silversmith RE. 2002. Structure and catalytic mechanism of the *E. coli* chemotaxis phosphatase CheZ. *Nat. Struct. Biol.* 9:570-75

124. Zhu X, Rebello J, Matsumura P, Volz K. 1997. Crystal structures of CheY mutants Y106W and T87I/Y106W: CheY activation correlates with movement of residue 106. *J. Biol. Chem.* 272:5000-06

125. Zhu Y, Qin L, Yoshida T, Inouye M. 2000. Phosphatase activity of histidine kinase EnvZ without kinase catalytic domain. *Proc. Natl. Acad. Sci. USA* 97:7808-13

PeerJ Preprints | https://doi.org/10.7287/peerj.preprints.27554v2 | CC BY 4.0 Open Access | rec: 21 Mar 2019, publ: 21 Mar 2019

TERMS AND DEFINITIONS

AcP	acetyl phosphate
BeF_3^-	beryllofluoride
CA	catalytic/ATP-binding (domain)
DBD	DNA-binding domain
DHp	dimerization/histidine phosphotransfer (domain)
ECF	extracytoplasmic function
HK	histidine kinase
HPt	histidine-containing phosphotransfer (domain)
PDB	Protein Data Bank
REC	receiver (domain of response regulator protein)
RR	response regulator protein
SDRR	single-domain response regulator
TCS	two-component system

PeerJ Preprints | https://doi.org/10.7287/peerj.preprints.27554v2 | CC BY 4.0 Open Access | rec: 21 Mar 2019, publ: 21 Mar 2019

FIGURE CAPTIONS

Figure 1. Common features of RRs. (***a***) Schematic diagram of the prototypical TCS pathway. (***b***) The conserved $(\beta\alpha)_5$ fold of REC domains. Phosphorylation site residues and the phosphoryl group mimic, beryllofluoride (BeF_3^-), are shown in sticks. (***c***) Sequence conservation of RECs. The profiled hidden Markov model (HMM) for the REC protein family (Pfam PF00072) is shown as sequence logos (113) with the secondary structure elements illustrated. Heights of individual stacked letters at each position correspond to information contents, reflecting the probability of observing the particular amino acids at each position. Phosphorylation site residues (stars), named after the most conserved amino acids (DD, D, T and K), are among the most conserved residues in REC domains.

Figure 2. Classification of RRs by their effector domains. The percentile distribution is indicated for RR effector functional classes and RR subfamilies. RR subfamilies are defined by effector domain folds identified in Pfam. Representative proteins are traditionally used to name the OmpR, NarL and NtrC subfamilies with effector domains named Trans_reg_C, GerE and Sigma54_activa in Pfam. Representative structures of each subfamily are shown with REC domains colored in grey and effector domains in colors (PDB ids: KdpE, 4KNY; RcsB, 5W43; LuxO, 5EP0; AgrA, 3BS1; AmiR, 1QO0; WspR, 3BRE; CheB, 1A2O).

Figure 3. Phosphorylation site of the REC domain. The phosphoryl group is positioned by a network of hydrogen bonds (dashed lines) with side chains of the highly conserved residues (orange) as well as backbone atoms of non-conserved residues (light pink). Non-conserved

PeerJ Preprints | https://doi.org/10.7287/peerj.preprints.27554v2 | CC BY 4.0 Open Access | rec: 21 Mar 2019, publ: 21 Mar 2019

936 active site residues are labeled by their relative sequence positions to the nearest conserved
937 residues, such as T+1, indicating one residue C-terminal to the conserved Thr/Ser residue. (***a***)
938 Phosphorylation site of the archetype RR CheY in the active conformation (PDB id: 1FQW) with
939 residues that are differently positioned in the inactive conformation (2CHE) shown in cyan. (***b***)
940 The putative trigonal bipyramidal transition state for both phosphorylation and
941 dephosphorylation. X represents the leaving group of the phosphodonor for phosphorylation or
942 the attacking water for dephosphorylation. (***c***) Surface view of the active site in the phosphatase-
943 REC complex (3HZH).

944

945 **Figure 4**. RR regulatory strategies. (***a***) Distinct inactive and active RR conformations
946 exemplified by full-length RR VraR (PDB ids: 4GVP, 4IF4). BeF_3^- is shown in red spheres. (***b***)
947 Schematic diagrams of RR regulatory mechanisms. Functional sites of effector domains, such as
948 enzyme sites or DNA recognition regions, are shown as pink dots. These sites can be buried or
949 exposed in a wide variety of inactive RR conformations and their activity depends on different
950 interactions between the REC and effector domains. Phosphorylation of the RR can relieve REC
951 domain inhibition, promote effector function or both. Representative RRs that utilize these
952 strategies are indicated.

953

954 **Figure 5**. Phosphorylation-induced conformational changes in the REC domain. RR structures
955 with or without BeF_3^- were aligned using the conserved strands β1, β3, β4, and β5 to compute the
956 average backbone RMSD per residue (***a***, *right*). RMSD values above the median + 2x MAD
957 (median absolute deviation) are considered as significant conformational changes and the

PeerJ Preprints | https://doi.org/10.7287/peerj.preprints.27554v2 | CC BY 4.0 Open Access | rec: 21 Mar 2019, publ: 21 Mar 2019

corresponding residues are colored blue. Non-REC structural elements are colored cyan. BeF_3^- is shown as red spheres and residues involved in the potential Y-T coupling are shown as green or gray sticks. Representative protein structures shown for the (***a***) Stand-alone, (***b***) OmpR, (***c***) NtrC and (***d***) NarL RR subfamilies are CheY (1F4V), DrrB (3NNS, 1P2F), NtrC1 (1ZY2, 1NY5) and VraR (4IF4). Y/T residues from the inactive CheY structure (2CHE) are differently positioned from the active structure. For the OmpR, NtrC and NarL subfamilies, two proteins from each subfamily were used for RMSD analyses and both showed similar regions of conformational changes. Substantial changes in α1 are also observed in one protein from the NtrC subfamily (pink).

Figure 6. Structure of the HK-RR complex. Ribbon (***a***) and surface (***b***) views of the HK856-RR468 complex (PDB id, 3DGE). Residues that determine the HK-RR interaction specificity (19, 96) are highlighted in light orange and cyan in the HK and RR, respectively. HK-RR contacts also involve other surface regions (grey), including both active sites of the HK (red) and the RR (pink).

PeerJ Preprints | https://doi.org/10.7287/peerj.preprints.27554v2 | CC BY 4.0 Open Access | rec: 21 Mar 2019, publ: 21 Mar 2019

Table 1. Dimerization modes and orientations of the conserved aromatic residue in RR subfamilies.

Family	P	Position of Y/F (inward)	Active Dimer Interface	Alt. Dimer Interfaces
OmpR	+	10/10[a]	**α4-β5-α5** (10/10) (1zes, 1xhf, 4uhk, 4s04, 6br7,…)	N.A.
	-	3/9 (MD) 9+3[b]/18(Rec)	**α4-β5-α5** (MD 3/9, Rec 16/18) (1xhe, 2hqr, 3nhz, 3r0j, 4kny, 4uhs,…)	**α1-α5** (2/27) (1b00, 4uhs) **Other** (1mvo)
NtrC	+	6/6	**α4-β5** (4/5) (1l5y, 1zy2, 2jrl, 4d6y)	**β5-α5** (1/5) (2vui)
	-	0/4 (MD) 2/7(Rec)	**α4-β5** (MD 0/4, Rec 2/7) (3cfy, 4d6x)	**β5-α5** (5/9) (1l5z, 2jk1, 3dzd, 4i4u, 5m7n)
NarL	+	8/8	**α1-α5** (7/8) (4if4, 4ldz, 4zmr, 5hev, 5o8z, 4e7p, 4le0)	**β6-α6** (6/8) (4if4, 4ldz, 4zmr, 5hev…) **α4-β5** (1/8) (1d5w)
	-	6/8 (MD) 7/8(Rec)	**α1-α5** (MD 4/8, Rec 5/8) (1rnl, 5vxn, 4hye, 4le1, 3eul, 3b2n…)	**β6-α6** (7/16) (4hye, 4le1, 2qsj, 5f64…) **α4-β5** (1/8) (1dbw)
LytTR	+/-[c]	1/1 (MD) 1/1(Rec)	**α4-loop-β5** (4cbv, 4ml3)	N.A.

a: Numbers are for individual protein fragments. The REC domain or multi-domain (MD) fragments of the same protein are individually counted.
b: Mixed positioning. Protein chains contain both inward and outward orientations of Y within a single crystal symmetry unit.
c: Phosphorylation status is mimicked with D to E or D to A mutations.

PeerJ Preprints | https://doi.org/10.7287/peerj.preprints.27554v2 | CC BY 4.0 Open Access | rec: 21 Mar 2019, publ: 21 Mar 2019

Figure 1

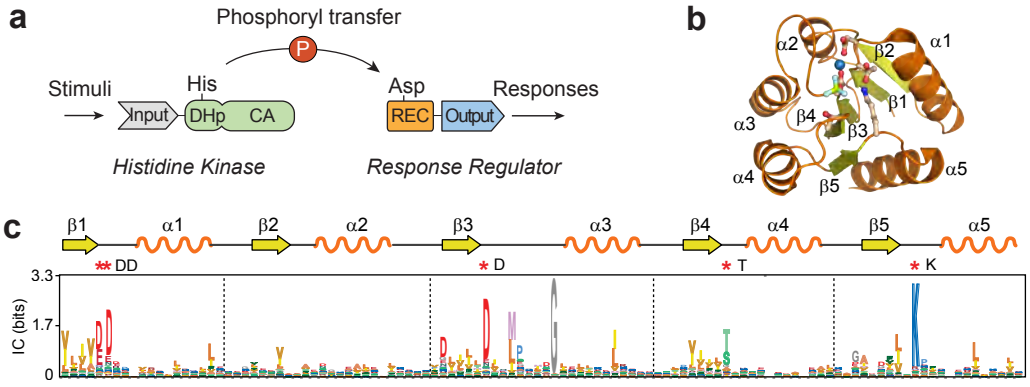
a
Phosphoryl transfer
P
Stimuli
His
Asp
Responses
Input
DHp
CA
REC
Output
Histidine Kinase
Response Regulator
b
α2
α1
β2
β1
α3
β4
β3
α4
β5
α5
c
β1
α1
β2
α2
β3
α3
β4
α4
β5
α5
** DD
* D
* T
* K
3.3
1.7
0
IC (bits)

Figure 2

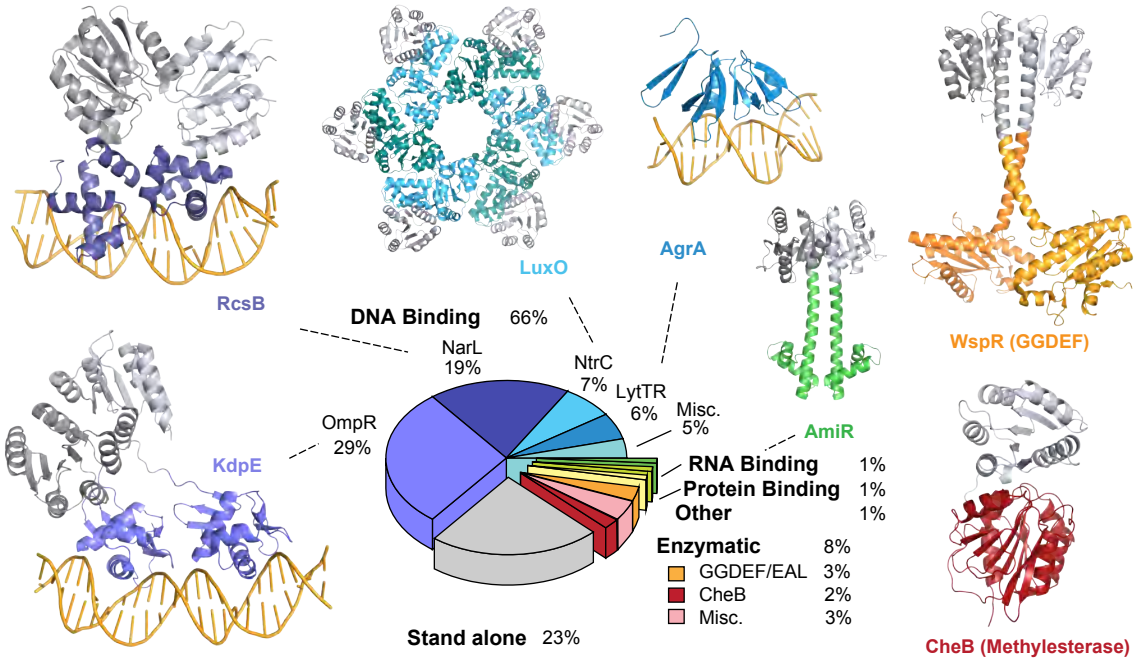
RcsB
LuxO
AgrA
WspR (GGDEF)
DNA Binding 66%
NarL 19%
NtrC 7%
LytTR 6%
Misc. 5%
OmpR 29%
KdpE
AmiR
RNA Binding 1%
Protein Binding 1%
Other 1%
Enzymatic 8%
GGDEF/EAL 3%
CheB 2%
Misc. 3%
Stand alone 23%
CheB (Methylesterase)

Figure 3

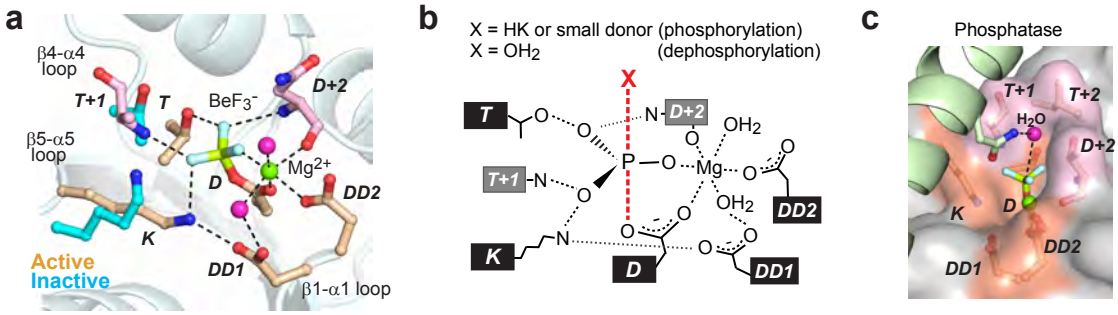

Figure 4

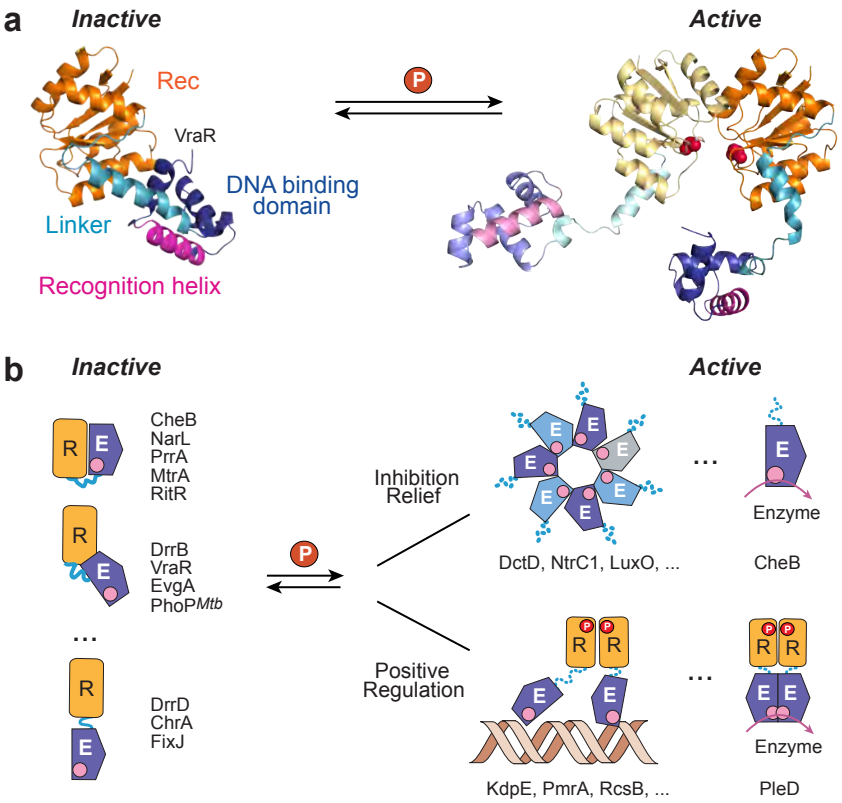
a
Inactive
Active
Rec
VraR
DNA binding domain
Linker
Recognition helix
P
b
Inactive
Active
CheB
NarL
PrrA
MtrA
RitR
DrrB
VraR
EvgA
PhoPMtb
DrrD
ChrA
FixJ
Inhibition Relief
Positive Regulation
DctD, NtrC1, LuxO, ...
CheB
Enzyme
KdpE, PmrA, RcsB, ...
PleD
Enzyme

Figure 5

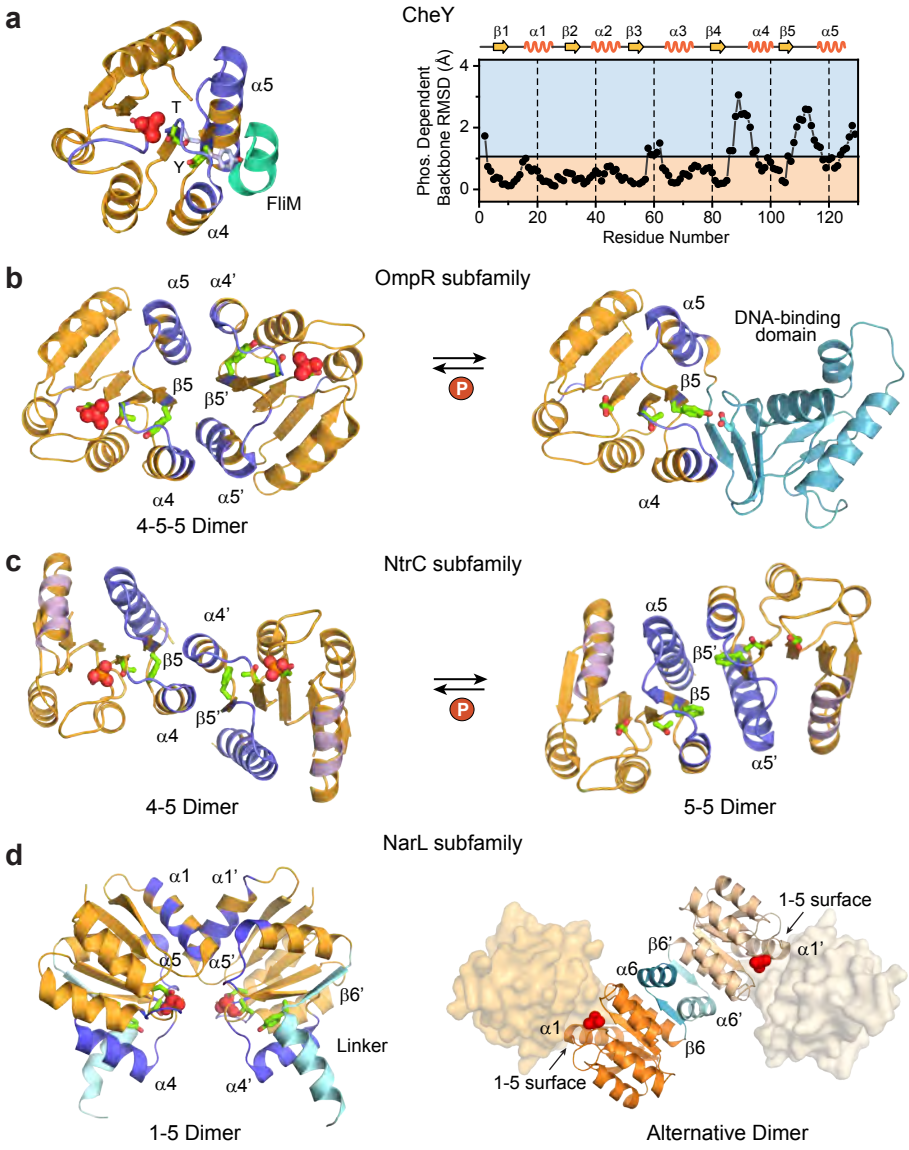

Figure 6